received 0.5% (w/v) hydroxypropylmethylcellulose as vehicle. Tumor volume was determined from caliper measurements of tumor length (L) and width (W) according to the formula $LW^2 / 2$. Both tumor size and body weight were measured two or three times per week.

Immunoblot Analysis

Cell lysates were fractionated by SDS-PAGE on 12% gels (NuPAGE Bis-Tris Gels; Invitrogen), and the separated proteins were transferred to a nitrocellulose membrane. After blocking of nonspecific sites with 5% skim milk, the membrane was incubated overnight at room temperature with primary antibodies. Antibodies to DPD, OPRT, and TS were obtained from Taiho Pharmaceutical; those to E2F-1 were from Santa Cruz Biotechnology; and those to β-actin (loading control) were from Sigma. Immune complexes were detected by incubation of the membrane for 1 h at room temperature with horseradish peroxidase–conjugated goat antibodies to mouse or rabbit immunoglobulin and by subsequent exposure to enhanced chemiluminescence reagents (Pierce).

Immunoprecipitation Analysis

Immunoprecipitation of EGFR was done according to standard procedures. Whole-cell lysates (800 μg protein) were incubated overnight at 4°C with antibodies to EGFR (Santa Cruz Biotechnology), after which Protein G Plus/Protein A-Agarose Suspension (Calbiochem) was added and the mixtures were incubated for an additional 1 h at 4°C. Immunoprecipitates were isolated, washed, resolved by SDS-PAGE on a 7.5% gel (Bio-Rad), and subjected to immunoblot analysis with antibodies to phosphotyrosine (PY20) and EGFR (Zymed).

Reverse Transcription and Real-time PCR Analysis

Total RNA (1 μg) extracted from cells with the use of an RNeasy Mini Kit (Qiagen) was subjected to reverse transcription with the use of a SuperScript Preamplification System (Invitrogen Life Technologies). The resulting cDNA was then subjected to real-time PCR analysis with the use of a TaqMan PCR Reagent Kit and a Gene Amp 5700 Sequence Detection System (Applied Biosystems). The forward and reverse primers and TaqMan probe for TS cDNA were 5-GCCTCGGTGTGCCTTTCA-3 and 5-CCCGTGATGTGCGCAAT-3 and 6-FAM-5′-TCGCCA-GCTACGCCCTGCTCA-3′-TAMRA, respectively. Glyceraldehyde-3-phosphate dehydrogenase mRNA were used as an internal standard.

Statistical Analysis

Data are presented as mean ± SE and were analyzed by the Aspin-Welch t test. $P < 0.05$ was considered statistically significant.

Results

Effect of the Combination of 5-FU and Gefitinib on NSCLC Cell Growth *In vitro*

Tegafur, which is a component of S-1, is metabolized to 5-FU in the liver and exerts antitumor effects. We first examined the antiproliferative activity of the combination of 5-FU and gefitinib in six NSCLC cell lines. Five of the cell lines (H460, Ma-53, Ma-45, Ma-31, and Ma-25) possess wild-type *EGFR* alleles, whereas Ma-1 cells harbor an *EGFR* mutation (E746_A750del) that is associated with a high response rate to the EGFR-TKIs gefitinib and erlotinib in individuals with advanced NSCLC. We assessed

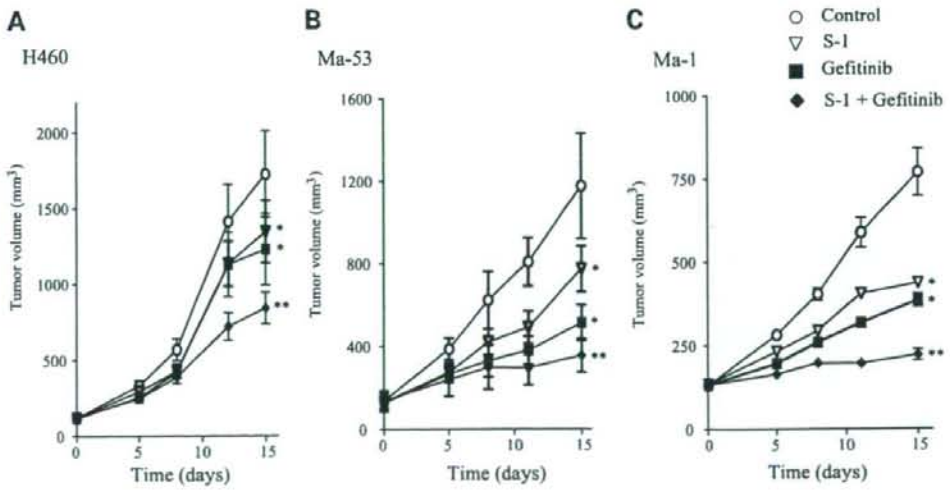

Figure 2. Antitumor activity of the combination of S-1 and gefitinib *in vivo*. **A** and **B**, nude mice with tumor xenografts established by s.c. implantation of NSCLC cells (H460 and Ma-53) possessing wild-type EGFR were treated daily for 2 wk with vehicle (control), S-1 (10 mg/kg), gefitinib (50 mg/kg), or both drugs by oral gavage. **C**, nude mice with tumor xenografts derived from NSCLC cells (Ma-1) expressing mutant EGFR were treated daily for 2 weeks with vehicle (control), S-1 (10 mg/kg), gefitinib (3 mg/kg), or both drugs by oral gavage. Tumor volume in all animals was determined at the indicated times after the onset of treatment. Mean ± SE of values from seven mice per group. *, $P < 0.05$ versus control; **, $P < 0.05$ versus S-1 or gefitinib alone for values 15 d after treatment onset (Aspin-Welch t test).

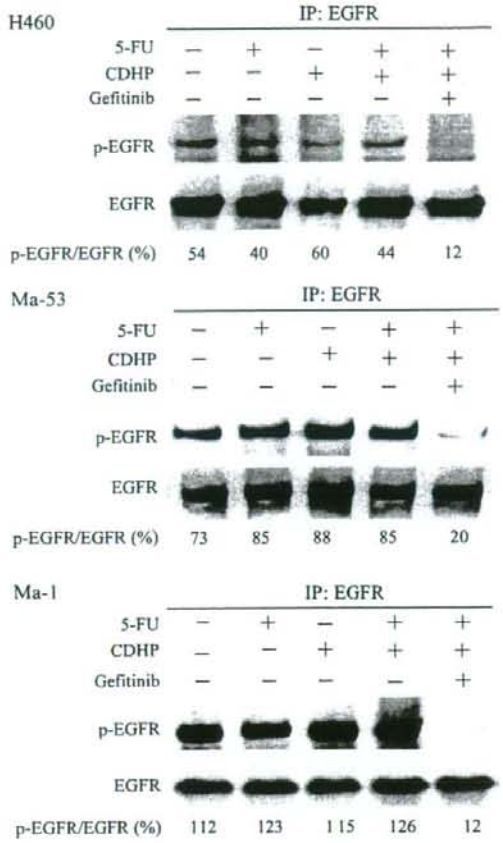

Figure 3. Lack of effect of 5-FU and CDHP on EGFR phosphorylation in NSCLC cell lines. NSCLC cells (H460, Ma-53, and Ma-1) were incubated for 24 h in medium supplemented with 2% fetal bovine serum and with 5-FU (10 μmol/L), CDHP (3 μmol/L), or gefitinib (5 μmol/L). Cell lysates were then prepared and subjected to immunoprecipitation (*IP*) with antibodies to EGFR, and the resulting precipitates were subjected to immunoblot analysis with antibodies to phosphotyrosine (for detection of phosphorylated EGFR) and with antibodies to EGFR. The intensity of the phosphorylated EGFR band relative to that of the EGFR band was determined by densitometry and is expressed as a percentage below each lane.

whether 5-FU and gefitinib showed additivity, synergy, or antagonism based on the Bliss additivism model (24–26). We chose this model rather than isobologram or combination index analysis because it would allow us to evaluate the nature of drug interactions even in instances in which the maximal inhibition by 5-FU or gefitinib alone was too low to obtain a reliable IC_{50} value. The six test concentrations for each agent were chosen after first determining the corresponding IC_{50} values. The IC_{50} values for 5-FU chemosensitivity were not associated with *EGFR* status and ranged from 7 to 11 μmol/L. The effect of combined treatment with 5-FU and gefitinib on the proliferation of the six NSCLC cell lines was tested in triplicate in a 6 × 6 concentration matrix. Calculation of the percentage inhibition in excess of that predicted by the Bliss additivism model revealed synergistic effects of Bliss > 0 for 5-FU and gefitinib in all of the six cell lines tested (Fig. 1). These results suggested that 5-FU and gefitinib act synergistically to inhibit cell growth in NSCLC cells.

Effect of Combined Treatment with S-1 and Gefitinib on NSCLC Cell Growth *In vivo*

We therefore next investigated whether combined treatment with S-1 and gefitinib might also exert a synergistic effect on NSCLC cell growth *in vivo*. Doses of both agents were selected so that their independent effects on tumor growth would be moderate. Nude mice were implanted s.c. with H460, Ma-53, or Ma-1 tumor fragments to establish tumor xenografts. When the H460 or Ma-53 tumors, which harbor wild-type *EGFR*, became palpable (100-150 mm^3), the mice were divided into four groups for daily treatment with vehicle, S-1 (10 mg/kg), gefitinib (50 mg/kg), or both drugs by oral gavage over 2 weeks. For xenografts formed by H460 or Ma-53 cells, combination therapy with S-1 and gefitinib resulted in a significant reduction in tumor size compared with that apparent in animals treated with S-1 or gefitinib alone (Fig. 2*A* and *B*). Mice bearing Ma-1 tumors, which express mutant *EGFR*, were treated with vehicle, S-1 (10 mg/kg), gefitinib (3 mg/kg), or both agents daily over 2 weeks. Combination treatment with S-1 and gefitinib significantly inhibited the growth of Ma-1 xenografts relative to that apparent in mice treated with either agent alone (Fig. 2*C*). None of the drug treatments induced a weight loss of >20% during the 2-week period, and no signs of overt drug toxicity were apparent (data not shown). These results thus suggested that combination chemotherapy with S-1 and gefitinib *in vivo* had a synergistic antitumor effect on NSCLC xenografts regardless of the absence or presence of *EGFR* mutations, consistent with our results *in vitro*.

Effects of 5-FU and CDHP on EGFR Phosphorylation in NSCLC Cell Lines

To investigate the mechanism responsible for the observed interaction between S-1 and gefitinib, we examined the effect of 5-FU on EGFR signal transduction in NSCLC cells expressing wild-type (H460 and Ma-53) or mutant (Ma-1) *EGFR*. Immunoprecipitation analysis revealed that exposure of H460 or Ma-53 cells to 5-FU (10 μmol/L) for 24 h had no effect on the basal level of EGFR phosphorylation (Fig. 3). We have shown previously that EGFR is constitutively phosphorylated in Ma-1 cells maintained in serum-free medium (23). Exposure of Ma-1 cells to 5-FU for 24 h did not affect this constitutive level of EGFR phosphorylation (Fig. 3). We next examined the effects of both CDHP, which is a component of S-1, and the combination of CDHP and 5-FU on EGFR phosphorylation in H460, Ma-53, and Ma-1 cells. Neither CDHP alone nor the combination of CDHP and 5-FU affected the level of EGFR phosphorylation in any of these three cell lines (Fig. 3). These results thus indicated that 5-FU and CDHP have no effect on EGFR signal transduction.

Effects of Gefitinib on the Expression of DPD, OPRT, and TS in NSCLC Cell Lines

We next investigated whether gefitinib might affect the expression of DPD, OPRT, or TS, enzymes that are major determinants of the sensitivity of cells to 5-FU. We first examined the abundance of these enzymes in the NSCLC cell lines H460, Ma-53, and Ma-1 by immunoblot analysis. The expression of DPD was detected in MiaPaca-2 cells (positive control) but not in H460, Ma-53, or Ma-1 cells (Fig. 4*A*). In contrast, OPRT and TS were detected in all three NSCLC cell lines and their abundance did not appear related to *EGFR* status (Fig. 4*A*). Treatment of H460, Ma-53, or Ma-1 cells with gefitinib (5 μmol/L) for up to 48 h resulted in a time-dependent decrease in the amount of TS, whereas that of OPRT or DPD remained unaffected (Fig. 4*B*). A reduced level of TS expression in tumors has been associated previously with a higher response rate to 5-FU-based chemotherapy (27, 28). Our data thus suggested that the suppression of TS expression by gefitinib might increase the sensitivity of NSCLC cells to 5-FU.

The transcription factor E2F-1 regulates expression of the TS gene (29–31). We therefore examined the possible effect of gefitinib on E2F-1 expression in NSCLC cell lines. Incubation of H460, Ma-53, or Ma-1 cells with gefitinib for up to 48 h also induced a time-dependent decrease in the amount of E2F-1 (Fig. 4*B*), suggesting that this effect might contribute to the down-regulation of TS expression by gefitinib in these cell lines.

Effect of Gefitinib on TS mRNA Abundance in NSCLC Cell Lines

The abundance of TS mRNA would be expected to be decreased if the down-regulation of E2F-1 expression by gefitinib was responsible for the reduced level of TS. We determined the amount of TS mRNA in H460, Ma-53, or Ma-1 cells at various times after exposure to gefitinib with the use of reverse transcription and real-time PCR analysis. Gefitinib indeed induced a time-dependent decrease in the amount of TS mRNA in all three NSCLC cell lines (Fig. 5), suggesting that the down-regulation of TS expression by gefitinib occurs at the transcriptional level and may be due to suppression of E2F-1 expression.

Discussion

The recent identification of activating somatic mutations of *EGFR* in NSCLC and their relevance to prediction of the therapeutic response to EGFR-TKIs such as gefitinib and erlotinib have had a major effect on NSCLC treatment (10–17). The response rate to these drugs remains low, however, in NSCLC patients with wild-tye *EGFR* alleles. Combination therapy with EGFR-TKIs and cytotoxic agents is a potential alternative strategy for NSCLC expressing wild-type *EGFR*. In the present study, we have evaluated the potential cooperative antiproliferative effect of combined treatment with the EGFR-TKI gefitinib and the new oral fluorouracil S-1 in NSCLC cell lines of differing *EGFR* status. We found that S-1 (or 5-FU) and gefitinib exert a synergistic antiproliferative effect on NSCLC cells both *in vivo* and *in vitro* regardless of the absence or presence of *EGFR* mutation. We chose a gefitinib dose of 50 mg/kg for treatment of mice bearing H460 or Ma-53 tumors. The median effective dose of gefitinib was shown previously to be ~50 mg/kg in athymic nude mice bearing A431 cell-derived xenografts (32). A gefitinib dose of 50 mg/kg has therefore subsequently been widely used in tumor xenograft studies (33–36). The U.S. Food and Drug Administration recommends that drug doses in animals be converted to those in humans based on body surface area (37). According to this guideline, a gefitinib dose of 50 mg/kg in mouse xenograft models is approximately equivalent to the therapeutic dose (250 mg/d) of the drug in humans. In addition, the tumor concentrations of gefitinib in NSCLC xenografts of mice treated with this drug (50 mg/kg) ranged from 9.7 to 13.3 μg/g, values that were similar to the

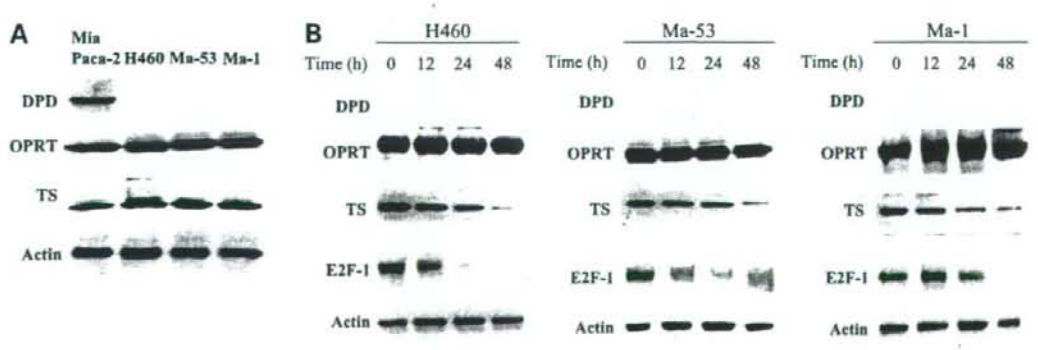

Figure 4. Effects of gefitinib on the expression of E2F-1, DPD, OPRT, and TS in NSCLC cell lines. **A**, lysates of H460, Ma-53, or Ma-1 cells were subjected to immunoblot analysis with antibodies to DPD, OPRT, TS, or β-actin (loading control). MiaPaca-2 cells were also examined as a positive control for DPD expression. **B**, NSCLC cells were incubated with gefitinib (5 μmol/L) for the indicated times in medium containing 10% serum, after which cell lysates were subjected to immunoblot analysis as in **A**, with the addition that E2F-1 expression was also examined.

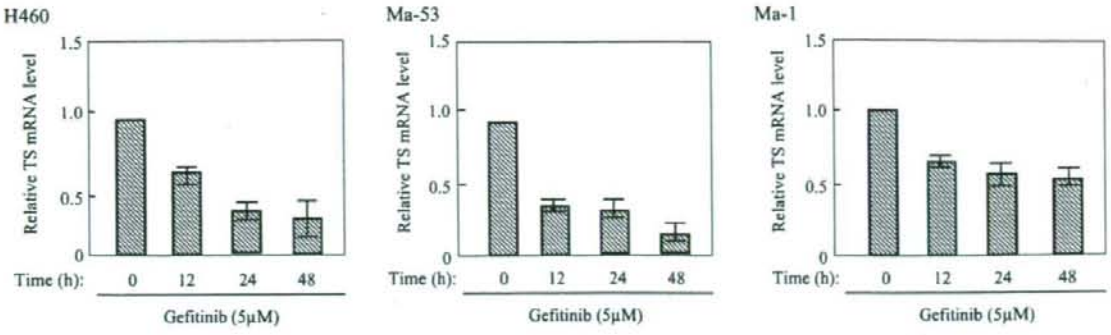

Figure 5. Down-regulation of TS mRNA by gefitinib in NSCLC cell lines. H460, Ma-53, or Ma-1 cells were incubated with gefitinib (5 μmol/L) for the indicated times in medium containing 10% serum, after which total RNA was extracted from the cells and subjected to reverse transcription and real-time PCR analysis of TS mRNA. The amount of TS mRNA was normalized by that of glyceraldehyde-3-phosphate dehydrogenase mRNA. Mean ± SE of values from three separate experiments.

achievable concentrations of gefitinib in tumor tissues of treated humans (34). These observations suggest that a gefitinib dose of 50 mg/kg in mouse xenograft models is appropriate for mimicking the therapeutic dose in humans.

EGFR-TKIs have been shown previously to act synergistically with radiation or cytotoxic agents such as cisplatin, paclitaxel, and irinotecan (38–40). These cytotoxic agents and radiation have been shown to increase the phosphorylation level of EGFR, possibly reflecting the activation of prosurvival signaling, and this effect is blocked by EGFR-TKIs, resulting in the synergistic antitumor effects of the combination therapies. Such a synergistic effect of 5-FU and gefitinib was attributed to 5-FU-induced EGFR phosphorylation in colorectal cancer cells (41). In contrast, we found that 5-FU had no effect on the level of EGFR phosphorylation in NSCLC cell lines. Further examination of different concentrations of 5-FU and different exposure times also failed to reveal an effect of 5-FU on EGFR phosphorylation in these cells (data not shown). These findings indicate that NSCLC cell lines respond differently to 5-FU than do colorectal cancer cells and that the synergistic antiproliferative effect of 5-FU and gefitinib in NSCLC cells is not mediated at the level of EGFR phosphorylation.

Our results indicate that the synergistic interaction of 5-FU (or S-1) and gefitinib is attributable, at least in part, to down-regulation of TS expression by gefitinib. The active metabolite of 5-FU, FdUMP, forms a covalent ternary complex with 5,10-methylenetetrahydrofolate and TS, resulting in inhibition of DNA synthesis (42). TS is thus an important therapeutic target of 5-FU. The amount of TS in neoplastic cells has been found to increase after exposure to 5-FU, resulting in the maintenance of free enzyme in excess of that bound to 5-FU (43–47). Such an increase in TS expression and activity has been viewed as a mechanistic driver of 5-FU resistance in cancer cells (48–50). The development of a new therapeutic strategy that reduces TS expression would therefore be of interest. Indeed, preclinical studies have shown that the down-regulation of TS by antisense oligonucleotides or other means enhances the efficacy of 5-FU (51–54). Down-regulation of TS would be expected to enhance the cytotoxicity of 5-FU as a result of the decrease in the amount of its protein target (55). Consistent with these preclinical data, an inverse relation between TS expression and 5-FU sensitivity has been shown in various human solid tumors (27, 28, 56–60). We have now shown that gefitinib alone induced down-regulation of TS expression, suggesting that this effect of gefitinib contributes to its synergistic interaction with 5-FU (or S-1) in NSCLC cell lines.

We further explored the molecular mechanism by which gefitinib induces down-regulation of TS expression in NSCLC cells. Given that EGFR signal transduction has been shown to be involved in activity of E2F-1 that regulates the expression of several genes including TS (61, 62), which controls the expression of several genes including that for TS, we examined the possible effects of gefitinib on E2F-1 expression and on the abundance of TS mRNA. Gefitinib induced down-regulation of E2F-1 in NSCLC cell lines harboring wild-type *EGFR*, consistent with previous observations (63), as well as in those expressing mutant *EGFR*. In addition, gefitinib reduced the amount of TS mRNA in NSCLC cells, consistent with the notion that the suppression of TS expression by gefitinib is attributable to inhibition of gene transcription as a result of down-regulation of E2F-1. For our experiments examining the effects of gefitinib on TS and E2F-1 expression, we used a drug concentration of 5 μmol/L. The concentration of gefitinib in tumor xenografts was shown previously to be 5 to 14 times that in the plasma concentration of the mouse hosts (34). Daily oral administration of gefitinib (250 mg) in patients also gave rise to a drug concentration in tumor tissue that was substantially higher (mean, 42-fold) than that in plasma concentration (34). We showed previously that the maximal concentration of gefitinib in the plasma of patients with advanced solid tumors had a mean value of 0.76 μmol/L at a daily dose of 225 mg (64). Based on these data, we considered that a gefitinib concentration of 5 μmol/L was appropriate for our

analyses of TS and E2F-1 expression. Together, our present findings suggest that down-regulation of E2F-1 and consequently that of TS by gefitinib is responsible, at least in part, for the synergistic antitumor effect of combined treatment with S-1 and gefitinib.

Somatic mutations of *EGFR* have been associated with sensitivity to EGFR-TKIs in patients with advanced NSCLC (13–16). However, although most NSCLCs with *EGFR* mutations initially respond to EGFR-TKIs, the vast majority of these tumors ultimately develop resistance to the drug. In the present study, the synergistic effect of combination chemotherapy with S-1 and gefitinib was observed even in *EGFR* mutant cells. Our findings thus suggest that the addition of S-1 (or 5-FU) to EGFR-TKIs might overcome chemoresistance to EGFR-TKIs and that exploration of the effect of such combination therapy in cells resistant to EGFR-TKIs is warranted. *EGFR* mutations appear to be largely limited to lung cancer, with few such mutations having been detected in other types of cancer (65–67). 5-FU is widely used as an anticancer agent and is considered a key drug in chemotherapy for solid tumors such as gastrointestinal and cervical cancer (68–70). Our present results show that gefitinib suppressed the expression of TS in NSCLC cell lines regardless of the absence or presence of *EGFR* mutations, suggesting that the addition of EGFR-TKIs to a 5-FU-containing regimen might increase the effectiveness of such treatment for solid cancers without *EGFR* mutations. Oral combined chemotherapy with drugs, such as S-1 and gefitinib, may also prove to be of low toxicity and therefore maintain quality of life. Our preclinical results provide a basis for future clinical investigations of combination chemotherapy with S-1 and EGFR-TKIs in patients with solid tumors.

References

1. Mendelsohn J, Baselga J. The EGF receptor family as targets for cancer therapy. Oncogene 2000;19:6550–65.
2. Schlessinger J. Cell signaling by receptor tyrosine kinases. Cell 2000; 103:211–25.
3. Hynes NE, Lane HA. ERBB receptors and cancer: the complexity of targeted inhibitors. Nat Rev Cancer 2005;5:341–54.
4. Hirsch FR, Varella-Garcia M, Bunn PA, Jr., et al. Epidermal growth factor receptor in non-small-cell lung carcinomas: correlation between gene copy number and protein expression and impact on prognosis. J Clin Oncol 2003;21:3798–807.
5. Suzuki S, Dobashi Y, Sakurai H, Nishikawa K, Hanawa M, Ooi A. Protein overexpression and gene amplification of epidermal growth factor receptor in nonsmall cell lung carcinomas. An immunohistochemical and fluorescence *in situ* hybridization study. Cancer 2005;103:1265–73.
6. Fukuoka M, Yano S, Giaccone G, et al. Multi-institutional randomized phase II trial of gefitinib for previously treated patients with advanced non-small-cell lung cancer (The IDEAL 1 Trial) [corrected]. J Clin Oncol 2003; 21:2237–46.
7. Perez-Soler R, Chachoua A, Hammond LA, et al. Determinants of tumor response and survival with erlotinib in patients with non-small-cell lung cancer. J Clin Oncol 2004;22:3238–47.
8. Thatcher N, Chang A, Parikh P, et al. Gefitinib plus best supportive care in previously treated patients with refractory advanced non-small-cell lung cancer: results from a randomised, placebo-controlled, multicentre study (Iressa Survival Evaluation in Lung Cancer). Lancet 2005;366:1527–37.
9. Shepherd FA, Rodrigues Pereira J, Ciuleanu T, et al. Erlotinib in previously treated non-small-cell lung cancer. N Engl J Med 2005;353: 123–32.
10. Lynch TJ, Bell DW, Sordella R, et al. Activating mutations in the epidermal growth factor receptor underlying responsiveness of non-small-cell lung cancer to gefitinib. N Engl J Med 2004;350:2129–39.
11. Paez JG, Janne PA, Lee JC, et al. EGFR mutations in lung cancer: correlation with clinical response to gefitinib therapy. Science 2004;304: 1497–500.
12. Pao W, Miller V, Zakowski M, et al. EGF receptor gene mutations are common in lung cancers from "never smokers" and are associated with sensitivity of tumors to gefitinib and erlotinib. Proc Natl Acad Sci U S A 2004;101:13306–11.
13. Mitsudomi T, Kosaka T, Endoh H, et al. Mutations of the epidermal growth factor receptor gene predict prolonged survival after gefitinib treatment in patients with non-small-cell lung cancer with postoperative recurrence. J Clin Oncol 2005;23:2513–20.
14. Takano T, Ohe Y, Sakamoto H, et al. Epidermal growth factor receptor gene mutations and increased copy numbers predict gefitinib sensitivity in patients with recurrent non-small-cell lung cancer. J Clin Oncol 2005;23: 6829–37.
15. Han SW, Kim TY, Hwang PG, et al. Predictive and prognostic impact of epidermal growth factor receptor mutation in non-small-cell lung cancer patients treated with gefitinib. J Clin Oncol 2005;23: 2493–501.
16. Tsao MS, Sakurada A, Cutz JC, et al. Erlotinib in lung cancer—molecular and clinical predictors of outcome. N Engl J Med 2005;353: 133–44.
17. Tokumo M, Toyooka S, Kiura K, et al. The relationship between epidermal growth factor receptor mutations and clinicopathologic features in non-small cell lung cancers. Clin Cancer Res 2005;11:1167–73.
18. Shirasaka T, Shimamoto Y, Fukushima M. Inhibition by oxonic acid of gastrointestinal toxicity of 5-fluorouracil without loss of its antitumor activity in rats. Cancer Res 1993;53:4004–9.
19. Tatsumi K, Fukushima M, Shirasaka T, Fujii S. Inhibitory effects of pyrimidine, barbituric acid and pyridine derivatives on 5-fluorouracil degradation in rat liver extracts. Jpn J Cancer Res 1987;78:748–55.
20. Shirasaka T, Shimamato Y, Ohshimo H, et al. Development of a novel form of an oral 5-fluorouracil derivative (S-1) directed to the potentiation of the tumor selective cytotoxicity of 5-fluorouracil by two biochemical modulators. Anticancer Drugs 1996;7:548–57.
21. Kawahara M, Furuse K, Segawa Y, et al. Phase II study of S-1, a novel oral fluorouracil, in advanced non-small-cell lung cancer. Br J Cancer 2001;85:939–43.
22. Ichinose Y, Yoshimori K, Sakai H, et al. S-1 plus cisplatin combination chemotherapy in patients with advanced non-small cell lung cancer: a multi-institutional phase II trial. Clin Cancer Res 2004;10:7860–4.
23. Okabe T, Okamoto I, Tamura K, et al. Differential constitutive activation of the epidermal growth factor receptor in non-small cell lung cancer cells bearing EGFR gene mutation and amplification. Cancer Res 2007;67:2046–53.
24. Berenbaum MC. Criteria for analyzing interactions between biologically active agents. Adv Cancer Res 1981;35:269–335.
25. Borisy AA, Elliott PJ, Hurst NW, et al. Systematic discovery of multicomponent therapeutics. Proc Natl Acad Sci U S A 2003;100:7977–82. Epub 2003 Jun 10.
26. Buck E, Eyzaguirre A, Brown E, et al. Rapamycin synergizes with the epidermal growth factor receptor inhibitor erlotinib in non-small-cell lung, pancreatic, colon, and breast tumors. Mol Cancer Ther 2006;5:2676–84.
27. Ichikawa W, Uetake H, Shirota Y, et al. Combination of dihydropyrimidine dehydrogenase and thymidylate synthase gene expressions in primary tumors as predictive parameters for the efficacy of fluoropyrimidine-based chemotherapy for metastatic colorectal cancer. Clin Cancer Res 2003;9:786–91.
28. Salonga D, Danenberg KD, Johnson M, et al. Colorectal tumors responding to 5-fluorouracil have low gene expression levels of dihydropyrimidine dehydrogenase, thymidylate synthase, and thymidine phosphorylase. Clin Cancer Res 2000;6:1322–7.
29. DeGregori J, Kowalik T, Nevins JR. Cellular targets for activation by the E2F1 transcription factor include DNA synthesis- and G_1/S-regulatory genes. Mol Cell Biol 1995;15:4215–24.
30. Dyson N. The regulation of E2F by pRB-family proteins. Genes Dev 1998;12:2245–62.
31. Trimarchi JM, Lees JA. Sibling rivalry in the E2F family. Nat Rev Mol Cell Biol 2002;3:11–20.

32. Wakeling AE, Guy SP, Woodburn JR, et al. ZD1839 (Iressa): an orally active inhibitor of epidermal growth factor signaling with potential for cancer therapy. Cancer Res 2002;62:5749 – 54.

33. Matar P, Rojo F, Cassia R, et al. Combined epidermal growth factor receptor targeting with the tyrosine kinase inhibitor gefitinib (ZD1839) and the monoclonal antibody cetuximab (IMC-C225): superiority over single-agent receptor targeting. Clin Cancer Res 2004;10:6487 – 501.

34. McKillop D, Partridge EA, Kemp JV, et al. Tumor penetration of gefitinib (Iressa), an epidermal growth factor receptor tyrosine kinase inhibitor. Mol Cancer Ther 2005;4:641 – 9.

35. Zhang X, Chen ZG, Choe MS, et al. Tumor growth inhibition by simultaneously blocking epidermal growth factor receptor and cyclo-oxygenase-2 in a xenograft model. Clin Cancer Res 2005;11:6261 – 9.

36. Haura EB, Zheng Z, Song L, Cantor A, Bepler G. Activated epidermal growth factor receptor-Stat-3 signaling promotes tumor survival *in vivo* in non-small cell lung cancer. Clin Cancer Res 2005;11:8288 – 94.

37. U S. Department of Health and Human Services, Food and Drug Administration, Center for Drug Evaluation and Research (CDER). Guidance for industry, estimating the maximum safe starting dose in initial clinical trials for therapeutics in adult healthy volunteers; 2005. p. 1 – 27.

38. Koizumi F, Kanzawa F, Ueda Y, et al. Synergistic interaction between the EGFR tyrosine kinase inhibitor gefitinib ("Iressa") and the DNA topoisomerase I inhibitor CPT-11 (irinotecan) in human colorectal cancer cells. Int J Cancer 2004;108:464 – 72.

39. Chinnaiyan P, Huang S, Vallabhaneni G, et al. Mechanisms of enhanced radiation response following epidermal growth factor receptor signaling inhibition by erlotinib (Tarceva). Cancer Res 2005;65:3328 – 35.

40. Van Schaeybroeck S, Kyula J, Kelly DM, et al. Chemotherapy-induced epidermal growth factor receptor activation determines response to combined gefitinib/chemotherapy treatment in non-small cell lung cancer cells. Mol Cancer Ther 2006;5:1154 – 65.

41. Van Schaeybroeck S, Karaiskou-McCaul A, Kelly D, et al. Epidermal growth factor receptor activity determines response of colorectal cancer cells to gefitinib alone and in combination with chemotherapy. Clin Cancer Res 2005;11:7480 – 9.

42. Peters GJ, van der Wilt CL, van Triest B, et al. Thymidylate synthase and drug resistance. Eur J Cancer 1995;31A:1299 – 305.

43. Spears CP, Shahinian AH, Moran RG, Heidelberger C, Corbett TH. *In vivo* kinetics of thymidylate synthetase inhibition of 5-fluorouracil-sensitive and -resistant murine colon adenocarcinomas. Cancer Res 1982;42:450 – 6.

44. Washtien WL. Increased levels of thymidylate synthetase in cells exposed to 5-fluorouracil. Mol Pharmacol 1984;25:171 – 7.

45. Spears CP, Gustavsson BG, Berne M, Frosing R, Bernstein L, Hayes AA. Mechanisms of innate resistance to thymidylate synthase inhibition after 5-fluorouracil. Cancer Res 1988;48:5894 – 900.

46. Swain SM, Lippman ME, Egan EF, Drake JC, Steinberg SM, Allegra CJ. Fluorouracil and high-dose leucovorin in previously treated patients with metastatic breast cancer. J Clin Oncol 1989;7:890 – 9.

47. Chu E, Zinn S, Boarman D, Allegra CJ. Interaction of γ interferon and 5-fluorouracil in the H630 human colon carcinoma cell line. Cancer Res 1990;50:5834 – 40.

48. Johnston PG, Drake JC, Trepel J, Allegra CJ. Immunological quantitation of thymidylate synthase using the monoclonal antibody TS 106 in 5-fluorouracil-sensitive and -resistant human cancer cell lines. Cancer Res 1992;52:4306 – 12.

49. Copur S, Aiba K, Drake JC, Allegra CJ, Chu E. Thymidylate synthase gene amplification in human colon cancer cell lines resistant to 5-fluorouracil. Biochem Pharmacol 1995;49:1419 – 26.

50. Kawate H, Landis DM, Loeb LA. Distribution of mutations in human thymidylate synthase yielding resistance to 5-fluorodeoxyuridine. J Biol Chem 2002;277:36304 – 11. Epub 2002 Jul 29.

51. Hsueh CT, Kelsen D, Schwartz GK. UCN-01 suppresses thymidylate synthase gene expression and enhances 5-fluorouracil-induced apoptosis in a sequence-dependent manner. Clin Cancer Res 1998;4:2201 – 6.

52. Ju J, Kane SE, Lenz HJ, Danenberg KD, Chu E, Danenberg PV. Desensitization and sensitization of cells to fluoropyrimidines with different antisenses directed against thymidylate synthase messenger RNA. Clin Cancer Res 1998;4:2229 – 36.

53. Lee JH, Park JH, Jung Y, et al. Histone deacetylase inhibitor enhances 5-fluorouracil cytotoxicity by down-regulating thymidylate synthase in human cancer cells. Mol Cancer Ther 2006;5:3085 – 95.

54. Wada Y, Yoshida K, Suzuki T, et al. Synergistic effects of docetaxel and S-1 by modulating the expression of metabolic enzymes of 5-fluorouracil in human gastric cancer cell lines. Int J Cancer 2006;119: 783 – 91.

55. Ferguson PJ, Collins O, Dean NM, et al. Antisense down-regulation of thymidylate synthase to suppress growth and enhance cytotoxicity of 5-FUdR, 5-FU and Tomudex in HeLa cells. Br J Pharmacol 1999;127: 1777 – 86.

56. Aaronson SA. Growth factors and cancer. Science 1991;254: 1146 – 53.

57. Johnston PG, Lenz HJ, Leichman CG, et al. Thymidylate synthase gene and protein expression correlate and are associated with response to 5-fluorouracil in human colorectal and gastric tumors. Cancer Res 1995; 55:1407 – 12.

58. Leichman CG, Lenz HJ, Leichman L, et al. Quantitation of intratumoral thymidylate synthase expression predicts for disseminated colorectal cancer response and resistance to protracted-infusion fluorouracil and weekly leucovorin. J Clin Oncol 1997;15:3223 – 9.

59. Pestalozzi BC, Peterson HF, Gelber RD, et al. Prognostic importance of thymidylate synthase expression in early breast cancer. J Clin Oncol 1997;15:1923 – 31.

60. Johnston PG, Mick R, Recant W, et al. Thymidylate synthase expression and response to neoadjuvant chemotherapy in patients with advanced head and neck cancer. J Natl Cancer Inst 1997;89:308 – 13.

61. Hanada N, Lo HW, Day CP, Pan Y, Nakajima Y, Hung MC. Co-regulation of B-Myb expression by E2F1 and EGF receptor. Mol Carcinog 2006;45:10 – 7.

62. Ginsberg D. EGFR signaling inhibits E2F1-induced apoptosis *in vivo*: implications for cancer therapy. Sci STKE 2007;pe4.

63. Suenaga M, Yamaguchi A, Soda H, et al. Antiproliferative effects of gefitinib are associated with suppression of E2F-1 expression and telomerase activity. Anticancer Res 2006;26:3387 – 91.

64. Nakagawa K, Tamura T, Negoro S, et al. Phase I pharmacokinetic trial of the selective oral epidermal growth factor receptor tyrosine kinase inhibitor gefitinib ("Iressa," ZD1839) in Japanese patients with solid malignant tumors. Ann Oncol 2003;14:922 – 30.

65. Barber TD, Vogelstein B, Kinzler KW, Velculescu VE. Somatic mutations of EGFR in colorectal cancers and glioblastomas. N Engl J Med 2004;351:2883.

66. Lee JW, Soung YH, Kim SY, et al. Absence of EGFR mutation in the kinase domain in common human cancers besides non-small cell lung cancer. Int J Cancer 2005;113:510 – 1.

67. Shigematsu H, Gazdar AF. Somatic mutations of epidermal growth factor receptor signaling pathway in lung cancers. Int J Cancer 2006;118: 257 – 62.

68. Herskovic A, Martz K, al-Sarraf M, et al. Combined chemotherapy and radiotherapy compared with radiotherapy alone in patients with cancer of the esophagus. N Engl J Med 1992;326:1593 – 8.

69. Vanhoefer U, Rougier P, Wilke H, et al. Final results of a randomized phase III trial of sequential high-dose methotrexate, fluorouracil, and doxorubicin versus etoposide, leucovorin, and fluorouracil versus infusional fluorouracil and cisplatin in advanced gastric cancer: a trial of the European Organization for Research and Treatment of Cancer Gastrointestinal Tract Cancer Cooperative Group. J Clin Oncol 2000;18:2648 – 57.

70. Gibson MK, Li Y, Murphy B, et al. Randomized phase III evaluation of cisplatin plus fluorouracil versus cisplatin plus paclitaxel in advanced head and neck cancer (E1395): an Intergroup Trial of the Eastern Cooperative Oncology Group. J Clin Oncol 2005;23:3562 – 7.

Phase II Study of Combination Therapy with S-1 and Irinotecan for Advanced Non–Small Cell Lung Cancer: West Japan Thoracic Oncology Group 3505

Isamu Okamoto,[1] Takashi Nishimura,[5] Masaki Miyazaki,[1] Hiroshige Yoshioka,[7] Akihito Kubo,[2] Koji Takeda,[3] Noriyuki Ebi,[8] Shunichi Sugawara,[9] Nobuyuki Katakami,[6] Masahiro Fukuoka,[4] and Kazuhiko Nakagawa[1]

Abstract

Purpose: To evaluate the efficacy and toxicity of combination therapy with the oral fluoropyrimidine formulation S-1 and irinotecan for patients with advanced NSCLC.

Experimental Design: Chemotherapy-naive patients with advanced NSCLC were treated with i.v. irinotecan (150 mg/m^2) on day 1 and with oral S-1 (80 mg/m^2) on days 1 to 14 every 3 weeks.

Results: Fifty-six patients (median age, 63 years; range, 40-74 years) received a total of 286 treatment cycles (median, 5; range, 1-15). No complete responses and 16 partial responses were observed, giving an overall response rate of 28.6% [95% confidence interval (95% CI), 17.3-42.2%]. Twenty-four patients (42.9%) had stable disease and 12 patients (21.4%) had progressive disease as the best response. The overall disease control rate (complete response + partial response + stable disease) was thus 71.4% (95% CI, 57.8-82.7%). Median progression-free survival was 4.9 months (95% CI, 4.0-6.4 months), whereas median overall survival was 15 months. Hematologic toxicities of grade 3 or 4 included neutropenia (25%), thrombocytopenia (3.6%), and anemia (3.6%), with febrile neutropenia being observed in four patients (7.1%). The most common nonhematologic toxicities of grade 3 or 4 included anorexia (14.3%), fatigue (8.9%), and diarrhea (8.9%). There were no deaths attributed to treatment.

Conclusions: The combination of S-1 and irinotecan is a potential alternative option with a favorable toxicity profile for the treatment of advanced NSCLC. This nonplatinum regimen warrants further evaluation in randomized trials.

Non–small cell lung cancer (NSCLC) is the leading cause of death related to cancer worldwide (1). Platinum-based chemotherapy is the standard first-line treatment for advanced NSCLC based on the moderate improvement in survival and quality of life it confers compared with best supportive care alone (2–4). The poor outlook even for patients with advanced NSCLC who receive such treatment has prompted a search for new chemotherapeutic agents and combination regimens.

S-1 is an oral fluorinated pyrimidine formulation that combines tegafur, 5-chloro-2,4-dihydroxypyridine (CDHP), and potassium oxonate in a molar ratio of 1:0.4:1 (5). Tegafur is a prodrug that generates 5-fluorouracil (5-FU) in blood largely as a result of its metabolism by cytochrome *P*450 in the liver. CDHP increases the plasma concentration of 5-FU through competitive inhibition of dihydropyrimidine dehydrogenase, which catalyzes 5-FU catabolism (6). CDHP also attenuates the cardiotoxic and neurotoxic effects of 5-FU by reducing the production of fluoro-β-alanine, the main catabolite of 5-FU (7, 8). Oxonate reduces the gastrointestinal toxicity of 5-FU. After its oral administration, oxonate becomes distributed selectively to the small and large intestine, where it inhibits the phosphorylation of 5-FU to fluoropyrimidine monophosphate catalyzed by orotate phosphoribosyltransferase within gastrointestinal mucosal cells, thereby reducing the incidence of diarrhea (9). In a phase II trial of S-1 as a single agent for treatment of advanced NSCLC, a response rate of 22% and a median survival time of 10.2 months were obtained in 59 patients without prior chemotherapy (10). Few severe gastrointestinal or hematologic adverse events were reported (10). Moreover, a phase II trial of S-1 plus cisplatin in advanced NSCLC patients revealed a response rate of 47% and a median survival time of 11 months (11).

Irinotecan is an inhibitor of DNA topoisomerase I. It has shown activity as a single agent in first-line chemotherapy for advanced NSCLC (12). Weekly administration of irinotecan

Authors' Affiliations: [1]Department of Medical Oncology, Kinki University School of Medicine; [2]Clinical Research Center, National Hospital Organization, Kinki-chuo Chest Medical Center; [3]Department of Clinical Oncology, Osaka City General Hospital; [4]Kinki University School of Medicine, Sakai Hospital, Osaka, Japan; [5]Department of Pulmonary Medicine, Kobe City General Hospital; [6]Division of Integrated Oncology, Institute of Biomedical Research and Innovation, Kobe, Japan; [7]Department of Respiratory Medicine, Kurashiki Central Hospital, Kurashiki, Japan; [8]Pulmonary Medicine, Iizuka Hospital, Iizuka, Japan; and [9]Pulmonary Medicine, Sendai Kousei Hospital, Sendai, Japan

Received 2/25/08; revised 3/29/08; accepted 4/14/08.

The costs of publication of this article were defrayed in part by the payment of page charges. This article must therefore be hereby marked *advertisement* in accordance with 18 U.S.C. Section 1734 solely to indicate this fact.

Requests for reprints: Isamu Okamoto, Department of Medical Oncology, Kinki University School of Medicine, 377-2 Ohno-higashi, Osaka-Sayama, Osaka 589-8511, Japan. Phone: 81-72-366-0221; Fax: 81-72-360-5000; E-mail: chi-okamoto@dotd.med.kindai.ac.jp.

doi:10.1158/1078-0432.CCR-08-0511

Translational Relevance

Non – small cell lung cancer (NSCLC) is the leading cause of cancer-related deaths worldwide. The dismal outlook for patients with advanced NSCLC treated with available therapies has prompted a search for new and more effective chemotherapeutic agents and combination regimens. S-1 is a new oral fluorinated pyrimidine formulation that combines tegafur, 5-chloro-2,4-dihydroxypyridine, and potassium oxonate and has been found to exhibit marked antitumor activity in recent clinical trials with cancer patients, including those with NSCLC. We have now examined the therapeutic efficacy and toxicity of the combination of S-1 and irinotecan in chemotherapy-naive patients with advanced NSCLC. We found this drug combination to be active, with a response rate of 28.6%, median progression-free survival of 4.9 months, and median overall survival of 15 months, values that compare favorably with those reported for phase III studies of standard platinum-based doublet chemotherapy. Furthermore, toxicities were manageable, and in most instances, treatment could be continued in the outpatient setting. Our data indicate that the combination of S-1 and irinotecan is a promising alternative for treatment of advanced NSCLC. This nonplatinum regimen warrants further evaluation in randomized trials.

(100 mg/m^2) for 3 weeks followed by 1 week of rest yielded a response rate of 20.5% and a median survival time of 10.6 months in 132 patients with advanced NSCLC (13).

S-1 and irinotecan have both shown single-agent activity against a wide range of solid tumors, including NSCLC, and the combination of these two agents has manifested synergistic effects in tumor xenograft models *in vivo* (14). A phase I study examined administration of irinotecan at a dose of 150 mg/m^2 on day 1 and of S-1 at 80 mg/m^2 per day from days 1 to 14 of a 21-day cycle (15); it found no difference in pharmacokinetic variables for the two drugs relative to the expected values for S-1 or irinotecan administered as single agents. A subsequent phase II study in patients with advanced colorectal cancer showed that this combination was well tolerated and had marked antitumor activity (16). The safety or effectiveness of the combination of S-1 and irinotecan in patients with advanced NSCLC has not previously been reported.

We now present the results of a multicenter phase II trial of S-1 in combination with irinotecan for patients with previously untreated advanced NSCLC. The aims of this study were to determine the objective tumor response rate, overall and progression-free survival, and toxicity profile for such treatment.

Materials and Methods

Patient eligibility. The criteria for patient eligibility included a diagnosis of NSCLC confirmed either histologically or cytologically, clinical stage IV or IIIB (including only patients with no indications for curative radiotherapy, such as those with malignant pleural effusion, pleural dissemination, malignant pericardial effusion, metastatic lesions in the same lobe of the primary lesion, or involvement of contralateral mediastinal or hilar lymph nodes), measurable disease, no prior chemotherapy, an age range of 20 to 74 y, an Eastern Cooperative Oncology Group performance status of 0 or 1, and a projected life expectancy of at least 3 mo. Other eligibility criteria for organ function included a leukocyte count of ≥3,000/mm^3, a neutrophil count of ≥1,500/mm^3, a platelet count of ≥100,000/μL, a serum bilirubin concentration of ≤1.5 mg/dL, serum aspartate aminotransferase (AST) and alanine aminotransferase (ALT) levels of ≤2.5 times the upper normal limit, a normal serum creatinine level, and either a partial pressure of arterial oxygen of ≥65 torr or a peripheral oxygen saturation of ≥92%. Main exclusion criteria included active concomitant of any malignancy, symptomatic brain metastasis, interstitial pneumonia, watery diarrhea, obstructive bowel disease, heart failure, uncontrolled diabetes mellitus, active infection, and a past history of drug allergy. Written informed consent was obtained from all patients, and the study protocol was approved by the institutional ethics committee of each of the participating institutions.

Study design and treatment. This was a multicenter, open-label, single-arm, phase II study. The primary end point of the study was the response rate, which determined the sample size. We chose a 35% response rate as a desirable target level and a 20% response rate as uninteresting with an α error of 0.05 and a power of 0.8, resulting in a requirement for 50 patients. Allowing for a patient ineligibility rate of 10%, we planned to enroll 55 patients.

Each treatment cycle consisted of the oral administration of S-1 (40 mg/m^2) twice daily for 2 wk, with a 90-min i.v. infusion of irinotecan (150 mg/m^2) on day 1 followed by a drug-free interval of 1 wk. S-1 was available as capsules containing 20 or 25 mg of tegafur. Patients were assigned based on body surface area to receive one of the following oral doses of S-1 twice daily: 40 mg (body surface area < 1.25 m^2), 50 mg (1.25 ≤ body surface area < 1.50 m^2), or 60 mg (body surface area ≥ 1.50 m^2). Courses of treatment were repeated every 21 d until the occurrence of tumor progression or unacceptable toxicity, refusal of the patient, or a decision by the physician to stop treatment.

If laboratory variables changed after the start of treatment so that they no longer met the eligibility criteria for the study, subsequent courses of treatment were withheld until the abnormality had resolved. If the abnormality had not resolved within 43 d, the patient was excluded from the study. The doses of both S-1 and irinotecan were reduced in the event of any of the following toxicities during the previous treatment cycle: neutropenia of grade 4 for >7 d, febrile neutropenia, thrombocytopenia of grade ≥4, and nonhematologic toxicity of grade ≥3. S-1 was reduced in subsequent courses from 60, 50, or 40 mg twice daily to 50, 40, and 25 mg twice daily, respectively. The dose of irinotecan was reduced by 25 mg/m^2 for subsequent courses. Once lowered, the doses of S-1 and irinotecan were not increased.

Evaluation. Tumor response was assessed according to the Response Evaluation Criteria in Solid Tumors (17). Tumors were measured by computed tomography within 2 wk before the first cycle of treatment and then every 4 wk. Patients were evaluable for response if they had a baseline exam and at least one follow-up exam and had received at least one cycle of treatment. A central radiological review was done to determine the eligibility of patients and the response to treatment. Response was confirmed at least 4 wk (for a complete or partial response) or 6 wk (for stable disease) after it was first documented. Progression-free survival was defined as the time from registration until objective tumor progression or death. Patients whose disease had not progressed at the time of discontinuation of the study treatment continued to be assessed until progression was documented. If a patient died without documentation of disease progression, the patients was considered to have had tumor progression at the time of death, unless there was sufficient documented evidence to conclude otherwise. Overall survival was defined as the time from registration until death from any cause. Progression-free and overall survival as well as the 1-y survival rate were estimated by the Kaplan-Meier method.

Table 1. Characteristics of the 56 eligible patients

Characteristic	No. patients
Median age, y (range)	63 (40-74)
Sex	
Male	46 (82%)
Female	10 (18%)
Performance status (ECOG)	
0	20 (36%)
1	36 (64%)
Stage	
IIIB	16 (29%)
IV	40 (71%)
Histology	
Adenocarcinoma	30 (54%)
Squamous cell carcinoma	21 (38%)
Adenosquamous cell carcinoma	1 (1.8%)
Large cell carcinoma	1 (1.8%)
NSCLC, not specified	3 (5.4%)

Abbreviation: ECOG, Eastern Cooperative Oncology Group.

Adverse events were graded according to the National Cancer Institute Common Toxicity Criteria (version 3). All patients who received one dose of chemotherapy were assessable for toxicity. A clinical and laboratory assessment was done at least every 2 wk.

Results

Patient characteristics. Between February and June 2006, a total of 59 patients were enrolled in the study at the 14 participating centers. Three patients did not receive treatment: one patient withdrew her consent, and two patients had a fall before treatment onset that resulted in a reduction in performance status. These three patients were thus not included in the analysis. The remaining 56 patients (46 men and 10 women) were eligible for the current analysis and their characteristics are summarized in Table 1. Their median age was 63 years, with a range of 40 to 74 years. Histologic analysis revealed that 30 patients (54%) had adenocarcinoma and 21 patients (38%) had squamous cell carcinoma. Forty patients (71%) had stage IV disease and the other 16 patients had stage IIIB disease (including 12 patients with malignant pleural effusion).

Treatment administered. Patients received a median of five cycles of treatment (range, 1-15), with 37 patients (66%) completing at least four cycles. Overall, 286 cycles of chemotherapy were delivered. The mean relative dose intensities of S-1 and irinotecan were 91% and 98%, respectively.

Table 2. Overall response rate (Response Evaluation Criteria in Solid Tumors criteria) by independent radiologic assessment

Response	No. patients (%)
Complete response	0 (0)
Partial response	16 (28.6)
Overall response	16 (28.6; 95% CI, 17.3-42.2)
Stable disease	24 (42.9)
Disease progression	12 (21.4)
Not evaluable	4 (7.1%)

Dose reductions were uncommon and were necessary according to the study protocol in only eight cycles (2.8% of total cycles) because of diarrhea in three patients, anorexia in two patients, vomiting in two patients, and an increase in serum ALT and AST levels in one patient. Treatment administration was delayed for at least 1 week because of toxicity in 12 cycles (4.2% of total cycles); the major causes of delayed administration were insufficient bone marrow function (six cycles with a leukocyte count of $<3{,}000/mm^3$ and one cycle with a platelet count of $<100{,}000/\mu L$) and nonhematologic toxicity (two cycles with fever in the absence of neutropenia, two cycles with an increase in serum ALT and AST levels, and one cycle with diarrhea).

Response and survival. Four patients were not evaluable for response: three patients withdrew from the study after one treatment cycle and one patient did not have a measurable target lesion. There were 16 partial responses and no complete responses, yielding an overall response rate of 28.6% (Table 2). Twenty-four patients (42.9%) had stable disease, yielding an overall disease control rate (complete response + partial response + stable disease) of 71.4% [95% confidence interval (95% CI), 57.8-82.7%]. Twelve patients (21.4%) had progressive disease as the best response.

All 56 treated patients were assessable for progression-free survival and overall survival. With a median follow-up time of 14.9 months (range, 1.4-20.1 months), 25 patients were still alive. The progression-free survival curve is shown in Fig. 1; the median progression-free survival was 4.9 months (95% CI, 4.0-6.4 months). The curve for overall survival is shown in Fig. 2; the median overall survival time was 15 months (95% CI could not be estimated) and the 1-year survival rate was 63% (95% CI, 50-75%). No correlation was apparent between overall survival and sex, age, histology, disease stage, or smoking status.

Toxicity. The adverse events observed for all 56 treated patients are summarized in Table 3. The most frequently observed hematologic toxicity of grade 3 or 4 was neutropenia (14 cases, 25%). Four patients (7.1%) developed febrile neutropenia. Anemia or thrombocytopenia of grade 3 or 4 was less frequent, each occurring in 3.6% of patients. Nonhematologic toxicities were generally mild in intensity. The most common nonhematologic toxicities of grade 3 or 4 were anorexia (14.3%), fatigue (8.9%), diarrhea (8.9%), vomiting (3.6%), and an increase in serum ALT or AST levels (3.6%). Treatment was discontinued because of toxicity in only two of

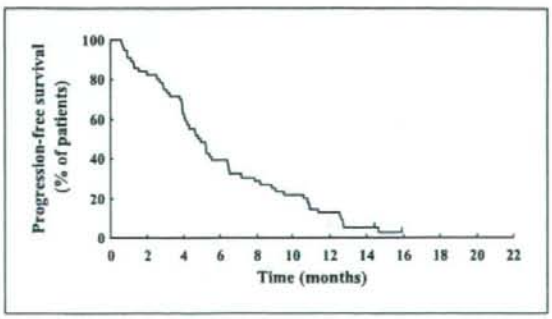

Fig. 1. Kaplan-Meier analysis of progression-free survival for all 56 treated patients.

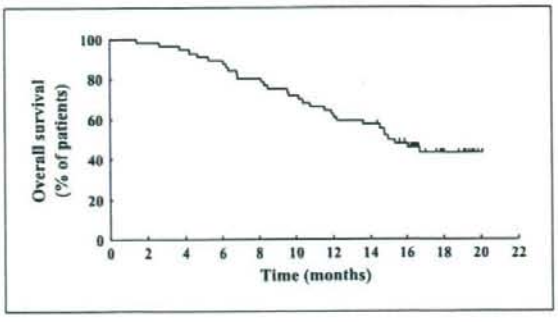

Fig. 2. Kaplan-Meier analysis of overall survival for all 56 treated patients.

the 56 patients (3.6%): in one patient because of pneumonitis (grade 3) and in the other because of prolonged anorexia (grade 3) and fatigue (grade 3). The patient with pneumonitis developed fever with hypoxemia after the fourth course of treatment. A computed tomographic scan of the chest revealed new ground-glass opacities distributed diffusely in both lungs. The patient responded well to steroid therapy and improved. No treatment-related deaths were observed.

Discussion

Platinum-based doublet chemotherapy is the standard of care for most patients with advanced NSCLC (2–4). However, there continues to be reluctance on the part of both patients and treating physicians to accept the toxicity of platinum-based therapy given the associated small gain in survival. Active therapies with improved toxicity profiles are clearly needed in this setting. Since the introduction of active third-generation agents (docetaxel, paclitaxel, gemcitabine, vinorelbine, and irinotecan), many clinical trials have been undertaken to evaluate nonplatinum regimens based on these drugs in the hope that platinum analogues could be eliminated from the treatment of advanced NSCLC. A recent meta-analysis showed that these newer nonplatinum regimens are valid options for the treatment of advanced NSCLC because of their shown activity and good toxicity profiles (18). Currently, however, there is no single best treatment regimen for advanced NSCLC.

As first-line chemotherapy for advanced NSCLC, the oral fluoropyrimidine formulation S-1 administered as a single agent showed a response rate of 22% and a median survival time of 10.2 months with toxicities that were generally mild (10). Combinations of S-1 with other active agents with a different mechanism of action are being investigated with the aim of achieving a greater clinical benefit. Irinotecan and fluoropyrimidines were shown not to induce cross-resistance in both experimental and clinical settings (19). Preclinical studies have also found that the combination of irinotecan and 5-FU has antitumor activities that are additive to synergistic (20). Furthermore, a possible molecular mechanism for synergistic cytotoxicity of S-1 and irinotecan has been suggested by the observation that irinotecan reduces thymidylate synthetase activity in tumor xenografts and thereby facilitates the antitumor effect of S-1 (14). Recent phase II studies have shown that combination treatment with S-1 and irinotecan is highly active with acceptable toxicity in patients with advanced colorectal cancer or gastric cancer (16, 21). However, the activity of this combination in patients with NSCLC has not previously been documented.

We have now assessed the efficacy and safety of combined treatment with S-1 and irinotecan in patients with previously untreated advanced NSCLC. We found the combination to be active, with a response rate of 28.6%, median progression-free survival of 4.9 months, median overall survival of 15 months, and 1-year survival rate of 63%. Previous phase III studies of platinum-based doublets for the treatment of advanced NSCLC showed response rates of 17% to 33%, a median time to progression or progression-free survival of 3 to 5 months, and a median overall survival time of 7 to 14 months (22–25). Although there are limitations to comparisons of the results from different studies, the efficacy data in our study compare favorably with those reported in these previous phase III studies of platinum-based doublets.

The S-1-irinotecan regimen was well tolerated in the patients of the present study. With regard to hematologic toxicity, neutropenia of grade 3 or 4 occurred in only 25% of all treated patients without the prophylactic administration of granulocyte colony-stimulating factor. Anemia and thrombocytopenia of grade 3 or 4 were each observed in only two patients (3.6%). These results compare favorably with the toxicity profiles reported for platinum-based combinations in previous studies with NSCLC patients, in which higher frequencies of neutropenia (~80%), anemia (~20%), and thrombocytopenia (~23%) of grade 3 or 4 were observed (22–24). The only nonhematologic toxicity of grade 3 or 4 encountered in >10% of patients in the present study was anorexia (14.3%). Although irinotecan and S-1 have each been shown to increase the frequency of severe diarrhea, the incidence of diarrhea of grade 3 in the present study was only 8.9%, consistent with the findings of a recent phase II study of the combination of S-1 and irinotecan administered according to the same doses and schedule in patients with advanced colorectal cancer (16).

Table 3. Toxicity for all 56 treated patients according to the National Cancer Institute Common Toxicity Criteria (version 3)

Toxicity	Grade				Grade ≥3 (%)
	1	2	3	4	
Leukopenia	9	10	5	0	8.9
Neutropenia	1	7	12	2	25.0
Anemia	31	19	1	1	3.6
Thrombocytopenia	23	2	2	0	3.6
Febrile neutropenia	NA	NA	4	0	7.1
Anorexia	25	10	8	0	14.3
Fatigue	18	12	4	1	8.9
Diarrhea	12	11	5	0	8.9
Nausea	27	11	1	0	1.8
Vomiting	12	4	2	0	3.6
Stomatitis	7	6	0	0	0
Rash	8	6	0	0	0
Hyperbilirubinemia	12	6	0	0	0
Elevation of AST/ALT	18	3	2	0	3.6
Elevation of creatinine	2	1	0	0	0
Pneumonitis	1	0	1	0	1.8

Abbreviation: NA, not applicable.

Thus, both hematologic and nonhematologic toxicities were generally manageable, and in most instances, treatment could be continued in an outpatient setting, resulting in a median of five treatment courses (range, 1-15).

In conclusion, we have presented the results of the first plhase II study of the combination of S-1 and irinotecan for the treatment of chemotherapy-naive patients with advanced NSCLC. This regimen yielded a response rate, progression-free survival, and overall survival similar to or better than those previously reported for platinum-based regimens. In addition, this regimen was well tolerated and could be administered in an outpatient setting. Given its efficacy and favorable toxicity profile, the combination of S-1 and irinotecan is a promising alternative for treatment of advanced NSCLC and a feasible nonplatinum option to which molecularly targeted agents can be added. The chemotherapy regimens of S-1 plus platinum derivatives have been studied (11). We are currently conducting a randomized phase III trial comparing carboplatin/S-1 with carboplatin/paclitaxel for chemonaive advanced NSCLC. We firmly believe that further trials comparing S-1 plus irinotecan with platinum-based doublet chemotherapy (perhaps carboplatin/S-1) are warranted.

Disclosure of Potential Conflicts of Interest

No potential conflicts of interest were disclosed.

Acknowledgments

We thank Koichi Hosoda for data management and Professor J. Patrick Barron of the International Medical Communications Center of Tokyo Medical University for his review of this manuscript.

References

1. Jemal A, Siegel R, Ward E, Murray T, Xu J, Thun MJ. Cancer statistics, 2007. CA Cancer J Clin 2007;57:43–66.
2. Chemotherapy in non-small cell lung cancer: a meta-analysis using updated data on individual patients from 52 randomised clinical trials. Non-small Cell Lung Cancer Collaborative Group. BMJ 1995;311:899–909.
3. Clinical practice guidelines for the treatment of unresectable non-small-cell lung cancer. Adopted on May 16, 1997 by the American Society of Clinical Oncology. J Clin Oncol 1997;15:2996–3018.
4. Socinski MA, Crowell R, Hensing TE, et al. Treatment of non-small cell lung cancer, stage IV: ACCP evidence-based clinical practice guidelines (2nd edition). Chest 2007;132:277–89S.
5. Shirasaka T, Nakano K, Takechi T, et al. Antitumor activity of 1 M tegafur-0.4 M 5-chloro-2,4-dihydroxypyridine-1 M potassium oxonate (S-1) against human colon carcinoma orthotopically implanted into nude rats. Cancer Res 1996;56:2602–6.
6. Takechi T, Nakano K, Uchida J, et al. Antitumor activity and low intestinal toxicity of S-1, a new formulation of oral tegafur, in experimental tumor models in rats. Cancer Chemother Pharmacol 1997;39:205–11.
7. Robben NC, Pippas AW, Moore JO. The syndrome of 5-fluorouracil cardiotoxicity. An elusive cardiopathy. Cancer 1993;71:493–509.
8. Kato T, Shimamoto Y, Uchida J, et al. Possible regulation of 5-fluorouracil-induced neuro- and oral toxicities by two biochemical modulators consisting of S-1, a new oral formulation of 5-fluorouracil. Anticancer Res 2001;21:1705–12.
9. Shirasaka T, Shimamoto Y, Fukushima M. Inhibition by oxonic acid of gastrointestinal toxicity of 5-fluorouracil without loss of its antitumor activity in rats. Cancer Res 1993;53:4004–9.
10. Kawahara M, Furuse K, Segawa Y, et al. Phase II study of S-1, a novel oral fluorouracil, in advanced non-small-cell lung cancer. Br J Cancer 2001;85:939–43.
11. Ichinose Y, Yoshimori K, Sakai H, et al. S-1 plus cisplatin combination chemotherapy in patients with advanced non-small cell lung cancer: a multi-institutional phase II trial. Clin Cancer Res 2004;10:7860–4.
12. Fukuoka M, Niitani H, Suzuki A, et al. A phase II study of CPT-11, a new derivative of camptothecin, for previously untreated non-small-cell lung cancer. J Clin Oncol 1992;10:16–20.
13. Negoro S, Masuda N, Takada Y, et al. Randomised phase III trial of irinotecan combined with cisplatin for advanced non-small-cell lung cancer. Br J Cancer 2003;88:335–41.
14. Takiuchi H, Narahara H, Tsujinaka T, et al. Phase I study of S-1 combined with irinotecan (CPT-11) in patients with advanced gastric cancer (OGSG 0002). Jpn J Clin Oncol 2005;35:520–5.
15. Yamada Y, Yasui H, Goto A, et al. Phase I study of irinotecan and S-1 combination therapy in patients with metastatic gastric cancer. Int J Clin Oncol 2003;8:374–80.
16. Goto A, Yamada Y, Yasui H, et al. Phase II study of combination therapy with S-1 and irinotecan in patients with advanced colorectal cancer. Ann Oncol 2006;17:968–73.
17. Therasse P, Arbuck SG, Eisenhauer EA, et al. New guidelines to evaluate the response to treatment in solid tumors. European Organization for Research and Treatment of Cancer, National Cancer Institute of the United States, National Cancer Institute of Canada. J Natl Cancer Inst 2000;92:205–16.
18. D'Addario G, Pintilie M, Leighl NB, Feld R, Cerny T, Shepherd FA. Platinum-based versus non-platinum-based chemotherapy in advanced non-small-cell lung cancer: a meta-analysis of the published literature. J Clin Oncol 2005;23:2926–36.
19. Vanhoefer U, Harstrick A, Achterrath W, Cao S, Seeber S, Rustum YM. Irinotecan in the treatment of colorectal cancer: clinical overview. J Clin Oncol 2001;19:1501–18.
20. Houghton JA, Cheshire PJ, Hallman JD II, et al. Evaluation of irinotecan in combination with 5-fluorouracil or etoposide in xenograft models of colon adenocarcinoma and rhabdomyosarcoma. Clin Cancer Res 1996;2:107–18.
21. Inokuchi M, Yamashita T, Yamada H, et al. Phase I/II study of S-1 combined with irinotecan for metastatic advanced gastric cancer. Br J Cancer 2006;94:1130–5.
22. Schiller JH, Harrington D, Belani CP, et al. Comparison of four chemotherapy regimens for advanced non-small-cell lung cancer. N Engl J Med 2002;346:92–8.
23. Fossella F, Pereira JR, von Pawel J, et al. Randomized, multinational, phase III study of docetaxel plus platinum combinations versus vinorelbine plus cisplatin for advanced non-small-cell lung cancer: the TAX 326 study group. J Clin Oncol 2003;21:3016–24.
24. Ohe Y, Ohashi Y, Kubota K, et al. Randomized phase III study of cisplatin plus irinotecan versus carboplatin plus paclitaxel, cisplatin plus gemcitabine, and cisplatin plus vinorelbine for advanced non-small-cell lung cancer: Four-Arm Cooperative Study in Japan. Ann Oncol 2007;18:317–23.
25. Hotta K, Fujiwara Y, Matsuo K, et al. Recent improvement in the survival of patients with advanced nonsmall cell lung cancer enrolled in phase III trials of first-line, systemic chemotherapy. Cancer 2007;109:939–48.

FEBS Letters 582 (2008) 4125–4130

The anti-EGFR monoclonal antibody blocks cisplatin-induced activation of EGFR signaling mediated by HB-EGF

Takeshi Yoshida[a], Isamu Okamoto[a,*], Tsutomu Iwasa[a], Masahiro Fukuoka[b], Kazuhiko Nakagawa[a]

[a] Department of Medical Oncology, Kinki University School of Medicine, 377-2 Ohno-higashi, Osaka-Sayama, Osaka 589-8511, Japan
[b] Kinki University School of Medicine, Sakai Hospital, 2-7-1 Harayamadai, Minami-ku Sakai, Osaka 590-0132, Japan

Received 21 July 2008; revised 2 October 2008; accepted 11 November 2008

Available online 21 November 2008

Edited by Richard Maras

Abstract **Cisplatin is a key agent in combination chemotherapy for various types of solid tumor. We now show that cisplatin activates signaling by the epidermal growth factor receptor (EGFR) by inducing cleavage of heparin-binding epidermal growth factor-like growth factor (HB-EGF). Matuzumab, a monoclonal antibody to EGFR, inhibited cisplatin-induced EGFR signaling, likely through competition with the soluble form of HB-EGF for binding to EGFR. Matuzumab enhanced the antitumor effect of cisplatin in nude mice harboring human non-small cell lung cancer xenografts. Our findings shed light on the mechanism by which monoclonal antibodies to EGFR might augment the efficacy of cisplatin.**

Keywords: EGF receptor; Heparin-binding EGF-like growth factor; Matuzumab; Cisplatin; Non-small cell lung cancer

1. Introduction

Cisplatin is a key component of combination chemotherapy for various types of solid tumor, but its effectiveness is limited by the development of chemoresistance [1]. Several nonphysiological stimuli that induce cellular stress, such as hyperosmolarity, wounding, UV or γ-radiation, reactive oxygen species, and chemotherapeutic agents, trigger activation of the epidermal growth factor receptor (EGFR) [2–11]. Ligand binding to EGFR induces receptor dimerization and activation of the receptor kinase, triggering intracellular signaling pathways such as those mediated by the protein kinases Akt or extracellular signal-regulated kinase (Erk), which play fundamental roles in the control of numerous cellular processes such as growth, proliferation, and survival [12–18]. EGFR signaling pathways activated by cellular stressors are thus of clinical interest because of their potential role in tumor resistance to chemotherapy [2–11]. The effects of cisplatin on EGFR signaling pathways have remained unclear, but the potential role of these pathways in cisplatin resistance makes it important to examine whether EGFR inhibitors might enhance the antitumor effects of this drug [8,9].

We have now examined the molecular mechanism of cisplatin-induced activation of EGFR and the effects of this drug on downstream signaling pathways. We also examined the effects of matuzumab (EMD72000, humanized mouse immunoglobulin G1), a monoclonal antibody (mAb) to EGFR [19], on cisplatin-dependent EGFR signaling. Finally, the antitumor effect of matuzumab combined with cisplatin was evaluated in order to provide insight into the mechanism by which anti-EGFR mAbs might augment the efficacy of cisplatin.

2. Materials and methods

2.1. Cell culture and reagents

The human non-small cell lung cancer (NSCLC) cell lines NCI-H292 (H292), NCI-H460 (H460), and A549 were obtained and cultured as previously described [20]. Matuzumab and gefitinib were also obtained as previously described [19]; GM6001 was from Calbiochem (La Jolla, CA); cisplatin, CRM197, and epidermal growth factor (EGF) were from Sigma (St. Louis, MO); and heparin-binding EGF-like growth factor (HB-EGF) was from R&D Systems (Minneapolis, MN).

2.2. Immunoblot analysis

Immunoblot analysis was performed as described previously [20]. Primary antibodies to the Tyr^{845}-phosphorylated form of EGFR, to EGFR, to phosphorylated Erk, to Erk, to phosphorylated Akt, and to Akt as well as horseradish peroxidase (HRP)-conjugated goat antibodies to mouse or rabbit immunoglobulin G were obtained as described previously [20]. Primary antibodies to the intracellular COOH-terminal domain of HB-EGF and HRP-conjugated donkey antibodies to goat immunoglobulin G were from Santa Cruz Biotechnology (Santa Cruz, CA).

2.3. Assessment of tumor growth inhibition in vivo

Tumor cells (2×10^6) were injected subcutaneously into the flank of 7-week-old female athymic nude mice. The mice were divided into four treatment groups of seven or eight animals: those treated over 2 weeks by intraperitoneal injection of vehicle, matuzumab (0.05 mg, twice per week), cisplatin (6 mg/kg of body weight, twice per week), or both matuzumab and cisplatin. Treatment was initiated when tumors in each group achieved an average volume of 200 mm^3, with tumor volume being determined twice weekly for 41 days after the onset of treatment from caliper measurement of tumor length (L) and width (W) according to the formula $LW^2/2$.

2.4. Ki67 index

Tumors were removed from some animals 14 days after treatment initiation and were stained with a mouse mAb to human Ki67 (clone MIB-1; Dako, Carpinteria, CA), as previously described [21]. The

*Corresponding author. Fax: +81 72 360 5000.
E-mail address: chi-okamoto@dotd.med.kindai.ac.jp (I. Okamoto).

Abbreviations: EGF, epidermal growth factor; EGFR, EGF receptor; mAb, monoclonal antibody; NSCLC, non-small cell lung cancer; HB-EGF, heparin-binding EGF-like growth factor; HRP, horseradish peroxidase; TUNEL, terminal deoxynucleotidyl transferase-mediated dUTP nick-end labeling

0014-5793/$34.00
doi:10.1016/j.febslet.2008.11.010

Ki67 index was determined as the percentage of Ki67-positive cells by scoring at least 300 tumor cells in each of 10 well-preserved fields of each tumor at a magnification of ×200 (CX41 light microscope; Olympus, Tokyo, Japan).

2.5. TUNEL staining

Terminal deoxynucleotidyl transferase-mediated dUTP nick-end labeling (TUNEL) analysis of tumor sections was performed as described previously [22]. The number of apoptotic cells in each of 10 fields (×200) per tumor was determined with a light microscope (CX41, Olympus).

2.6. Statistical analysis

Quantitative data are presented as means ± S.D. and were compared among groups by one-way analysis of variance followed by Tukey's multiple comparison test. A P value of <0.05 was considered

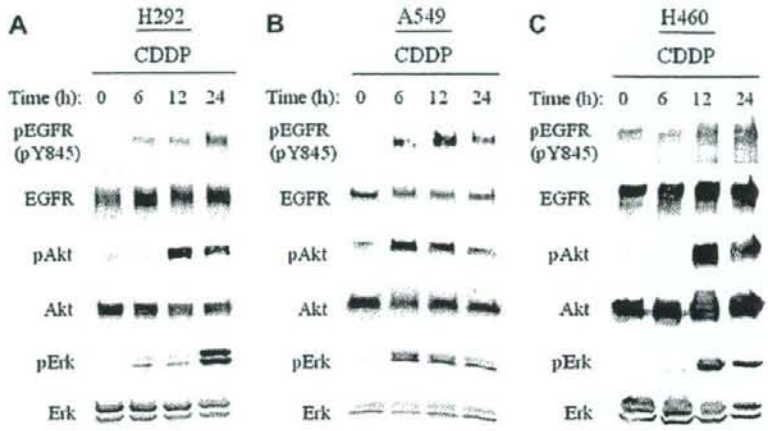

Fig. 1. Cisplatin-induced activation of EGFR and of downstream signaling pathways mediated by Akt or Erk. Serum-deprived H292 (A), A549 (B), or H460 (C) cells were incubated for the indicated times in the absence or presence of cisplatin (CDDP, 100 μM). Cell lysates were then subjected to immunoblot analysis with antibodies to the Tyr^{845}-phosphorylated form of EGFR (pEGFR), to phosphorylated Akt, or to phosphorylated Erk as well as with antibodies to total forms of these proteins.

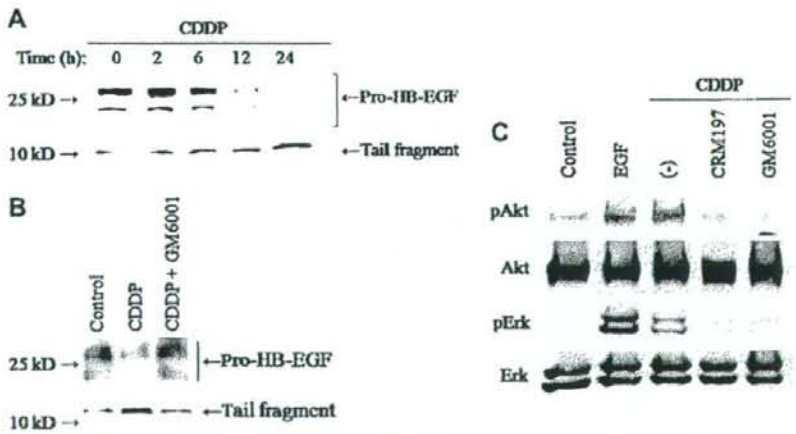

Fig. 2. Cisplatin-induced HB-EGF cleavage and its role in activation of EGFR signaling pathways by cisplatin. (A) Serum-deprived H292 cells were incubated for the indicated times in the presence of cisplatin (100 μM). Cell lysates were then subjected to immunoblot analysis with antibodies to the intracellular COOH-terminal domain of HB-EGF. The positions of molecular size standards (left) as well as of bands corresponding to pro-HB-EGF and to the cleaved tail fragment (right) are indicated. (B) Serum-deprived H292 cells were incubated alone (control) or with cisplatin (100 μM) in the absence or presence of GM6001 (10 μM) for 12 h. Cell lysates were then subjected to immunoblot analysis as in (A). (C) Serum-deprived H292 cells were incubated with EGF (100 ng/ml) for 15 min as a positive control or with cisplatin (100 μM) in the absence or presence of GM6001 (10 μM) or CRM197 (10 μg/ml) for 12 h. Cell lysates were then subjected to immunoblot analysis with antibodies to phosphorylated or total forms of Akt or Erk.

statistically significant. Statistical analysis was performed with GraphPad Prism version 5.00 for Windows (GraphPad Software, San Diego, CA).

3. Results and discussion

3.1. Cisplatin activates EGFR as well as downstream Akt and Erk signaling pathways

Cellular stress induced by several chemotherapeutic agents or γ-radiation triggers the activation of EGFR signaling pathways, with this effect being thought to play an important role in resistance to chemotherapy or radiotherapy [6–11]. We examined the effects of cisplatin on EGFR and downstream signaling pathways mediated by Akt or Erk in human NSCLC cell lines (H292, A549, H460). Cisplatin induced the phosphorylation of EGFR, Akt, and Erk in a time-dependent manner, without affecting the total amounts of these proteins, in all three cell lines (Fig. 1). These results thus showed that cisplatin activates EGFR and downstream signaling pathways mediated by Akt or Erk.

3.2. Cisplatin activates EGFR signaling pathways by inducing the cleavage of HB-EGF

HB-EGF is a membrane-bound EGFR ligand that activates EGFR after its release from the membrane in response to cellular stress [3,5,23–25]. To determine whether HB-EGF contributes to cisplatin-induced EGFR signaling, we examined the possible effect of cisplatin on cleavage of the membrane-bound pro-form of HB-EGF in H292 cells. Cisplatin induced a time-dependent decrease in the amount of pro-HB-EGF and a consequent increase in the amount of a COOH-terminal fragment of this protein referred to as the "tail fragment" (Fig. 2A). These effects of cisplatin were inhibited by GM6001 (Fig. 2B), a potent inhibitor of matrix metalloproteinases responsible for HB-EGF cleavage [23,24], suggesting that cisplatin induces metalloproteinase-mediated cleavage of the ectodomain of HB-EGF and its release from the cell sur-

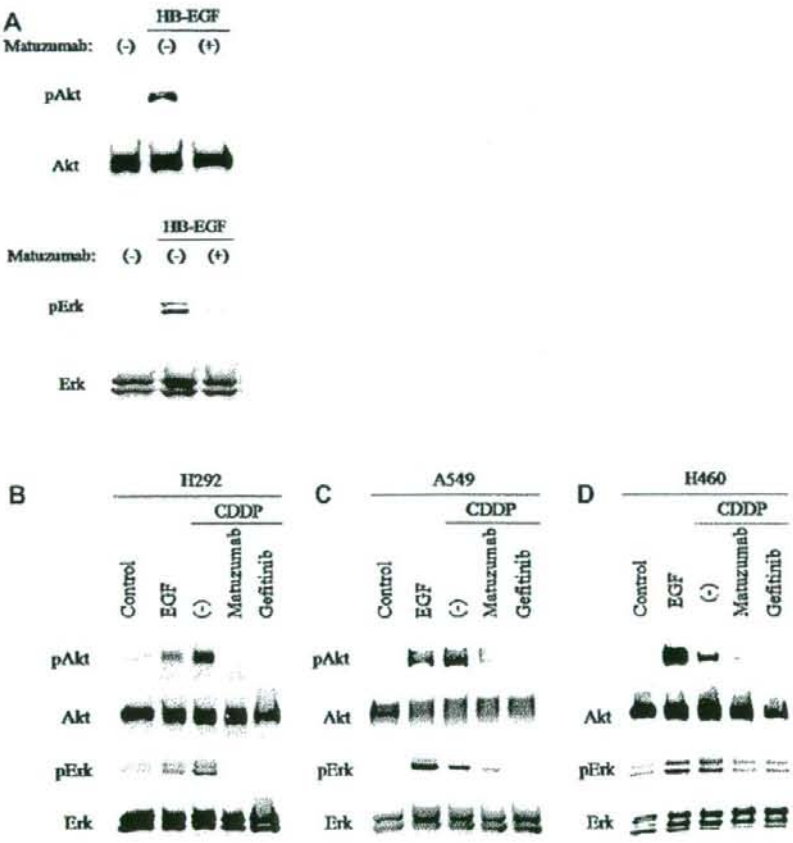

Fig. 3. Inhibition by matuzumab of EGFR signaling induced by HB-EGF or by cisplatin. (A) Serum-deprived H292 cells were incubated first for 2 h in the absence or presence of matuzumab (200 nM) and then for 15 min in the additional absence or presence of HB-EGF (10 ng/ml). Cell lysates were then subjected to immunoblot analysis with antibodies to phosphorylated or total forms of Akt or Erk. (B–D) Serum-deprived H292 (B), A549 (C), or H460 (D) cells were incubated with EGF (100 ng/ml) for 15 min as a positive control or with cisplatin (100 μM) in the absence or presence of matuzumab (200 nM) or gefitinib (10 μM) for 12 h. Cell lysates were then subjected to immunoblot analysis as in (A).

face. GM6001 also blocked the activation of Akt and Erk by cisplatin (Fig. 2C), implicating HB-EGF cleavage in cisplatin-induced EGFR signaling. To explore further whether cisplatin-induced EGFR signaling is dependent on HB-EGF activity, we examined the effect of CRM197, a nontoxic mutant form of diphtheria toxin that binds specifically to and neutralizes HB-EGF, which has also been identified as a diphtheria toxin receptor [26]. CRM197 completely inhibited the activation of Akt and Erk by cisplatin (Fig. 2C), suggesting that cisplatin promotes EGFR signaling by inducing the cleavage of HB-EGF. Consistent with this notion, the time course of cisplatin-induced activation of EGFR signaling (Fig. 1A) was similar to that of cisplatin-induced release of HB-EGF from the cell surface (Fig. 2A).

Cisplatin has previously been shown to increase the amount of HB-EGF mRNA in various types of cancer cells [7], and expression of the HB-EGF gene was found to be increased in cisplatin-resistant cancer [27]. The chemotherapeutic drugs SN38, doxorubicin, and imatinib also induce EGFR signaling and subsequent chemoresistance through metalloproteinase-dependent cleavage of HB-EGF [7,10]. It is possible that EGFR signaling resulting from metalloproteinase-mediated cleavage of HB-EGF represents a common mechanism of cellular resistance to various chemotherapeutic agents.

3.3. Effects of matuzumab on cisplatin-induced EGFR signaling

The clinical efficacy of treatment with anti-EGFR mAbs has been thought to be due to their prevention of ligand binding to EGFR [28,29]. We hypothesized that anti-EGFR mAbs might inhibit cisplatin-induced EGFR signaling by blocking the binding of the released ectodomain of HB-EGF to EGFR. To test whether anti-EGFR mAbs inhibit EGFR signaling induced by HB-EGF, we examined the effects of the humanized anti-EGFR mAb matuzumab. Matuzumab indeed prevented the activation of Akt and Erk by HB-EGF (Fig. 3A), indicating that this mAb inhibits HB-EGF–dependent EGFR signaling. We next examined the effect of matuzumab on cisplatin-induced EGFR signal transduction. The activation of EGFR downstream signaling by cisplatin was abolished by gefitinib in H292, A549, and H460 cells (Fig. 3B–D), suggesting that cisplatin-induced EGFR signaling requires the tyrosine kinase activity of EGFR. Matuzumab also markedly inhibited

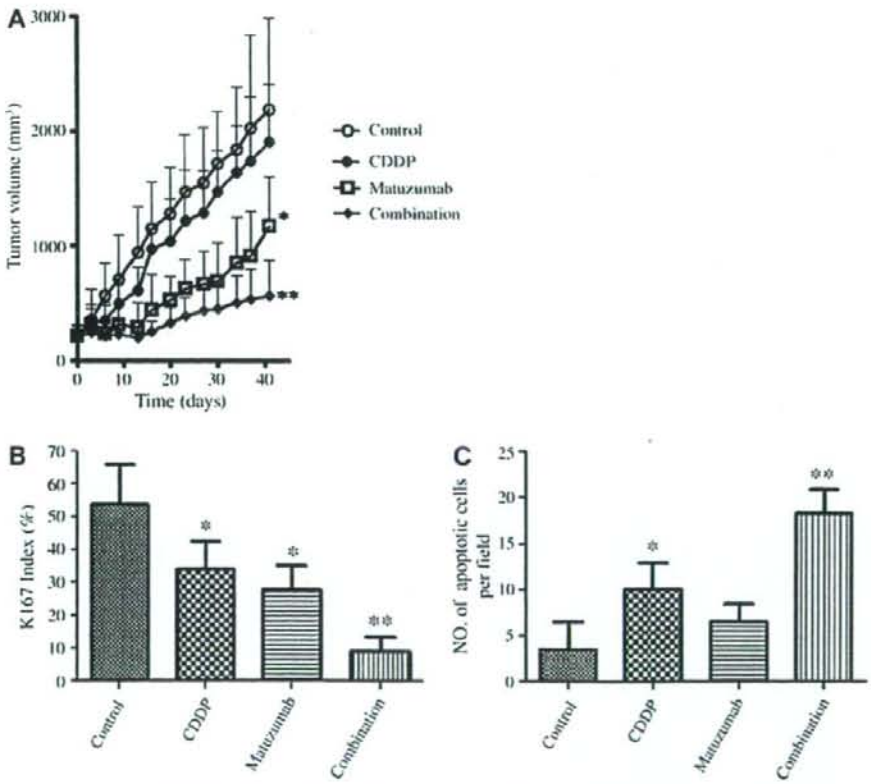

Fig. 4. Enhancement by matuzumab of the antitumor effect of cisplatin in vivo. (A) Nude mice harboring H292 tumor xenografts (200 mm^3) were treated with a single intraperitoneal dose of matuzumab (0.05 mg) or cisplatin (6 mg/kg), with both agents, or with vehicle (control) twice a week for 14 days. Tumor volume was determined at the indicated times after the onset of treatment. (B) The Ki67 index was determined from sections of H292 tumor xenografts 14 days after the initiation of treatment as in (A). (C) Quantitation by TUNEL staining of the number of apoptotic cells per field (×200) in H292 tumor xenografts 14 days after the initiation of treatment as in (A). Data in (A–C) are means ± S.D. $^*P < 0.05$ versus control; $^{**}P < 0.05$ versus control or each agent alone.

cisplatin-induced EGFR signaling in all three cell lines (Fig. 3B–D). These results thus suggested that matuzumab blocks cisplatin-induced EGFR signaling through inhibition of HB-EGF-dependent activation of EGFR.

Matuzumab exerts its antitumor effect both by competition with EGF for binding to EGFR and by blockade of the EGFR turnover that is important for activation of downstream signaling pathways mediated by Akt or Erk [19,28,29]. The soluble form of HB-EGF includes the EGF-like domain, a common structure in members of the EGF family of proteins that consists of 40–45 amino acids and contains six cysteine residues, but it binds not only to EGFR but also to ErbB4, whereas EGF binds specifically to EGFR [23–25]. The corresponding binding site of EGFR or the ligand function of HB-EGF may therefore differ from those for EGF. Nevertheless, we have now shown that matuzumab also inhibits the activation of EGFR signaling by both HB-EGF and cisplatin.

3.4. Matuzumab enhances the antitumor action of cisplatin in H292 xenografts

If cisplatin-induced EGFR signaling plays an important role in the development of cisplatin resistance, matuzumab might be expected to enhance the antitumor effect of cisplatin by inhibiting such signaling. We therefore determined the efficacy of combined treatment with matuzumab and cisplatin in nude mice with solid tumors formed by H292 cells injected into the flank. Combination therapy with matuzumab and cisplatin inhibited tumor growth to a significantly greater extent than did treatment with matuzumab or cisplatin alone (Fig. 4A).

Tumors treated with the combination of matuzumab and cisplatin also manifested both a significantly smaller Ki67 index (Fig. 4B), a marker of cell proliferation, and a significantly greater proportion of apoptotic cells (Fig. 4C), compared with tumors treated with either agent alone. Matuzumab alone or in combination with cytotoxic agents was previously shown to inhibit Akt or Erk phosphorylation in human tissue samples or human xenografts in nude mice [30–34]. The combination of matuzumab and cisplatin likely reduced the Ki67 index in the present study because matuzumab blocked the cisplatin-induced activation of Erk, which is important for cancer cell proliferation as a component of the Ras-MEK-Erk signaling pathway [17,18]. The increase in the number of apoptotic cells in tumors treated with both matuzumab and cisplatin likely resulted from inhibition by matuzumab of the cisplatin-induced activation of Akt, which contributes to antiapoptotic signaling through several pathways [15,16]. Our data thus indicate that matuzumab enhanced the antitumor effect of cisplatin, with the combination treatment inhibiting tumor cell proliferation and inducing apoptosis to a greater extent than treatment with either agent alone. Our data showing that gefitinib also blocked cisplatin-induced activation of Akt and Erk may explain the previous observation that the growth-inhibitory action of cisplatin in A549 tumors was increased fourfold in combination with gefitinib [35]. Our findings suggest the importance of EGFR signaling in the development of chemoresistance to cisplatin, and they provide insight into the mechanism by which anti-EGFR mAbs might augment the efficacy of cisplatin. Clinical studies of the therapeutic efficacy of matuzumab combined with cisplatin are thus warranted.

Acknowledgments: We thank Erina Hatashita, Yuki Yamada, and Takeko Wada for technical assistance.

References

[1] Siddik, Z.H. (2003) Cisplatin: mode of cytotoxic action and molecular basis of resistance. Oncogene 22, 7265–7279.
[2] El-Abaseri, T.B., Putta, S. and Hansen, L.A. (2006) Ultraviolet irradiation induces keratinocyte proliferation and epidermal hyperplasia through the activation of the epidermal growth factor receptor. Carcinogenesis 27, 225–231.
[3] Xu, K.P., Ding, Y., Ling, J., Dong, Z. and Yu, F.S. (2004) Wound-induced HB-EGF ectodomain shedding and EGFR activation in corneal epithelial cells. Invest. Ophthalmol. Vis. Sci. 45, 813–820.
[4] King, C.R., Borrello, I., Porter, L., Comoglio, P. and Schlessinger, J. (1989) Ligand-independent tyrosine phosphorylation of EGF receptor and the erbB-2/neu proto-oncogene product is induced by hyperosmotic shock. Oncogene 4, 13–18.
[5] Chen, C.H., Cheng, T.H., Lin, H., Shih, N.L., Chen, Y.L., Chen, Y.S., Cheng, C.F., Lian, W.S., Meng, T.C., Chiu, W.T. and Chen, J.J. (2006) Reactive oxygen species generation is involved in epidermal growth factor receptor transactivation through the transient oxidization of Src homology 2-containing tyrosine phosphatase in endothelin-1 signaling pathway in rat cardiac fibroblasts. Mol. Pharmacol. 69, 1347–1355.
[6] Park, C.M., Park, M.J., Kwak, H.J., Lee, H.C., Kim, M.S., Lee, S.H., Park, I.C., Rhee, C.H. and Hong, S.I. (2006) Ionizing radiation enhances matrix metalloproteinase-2 secretion and invasion of glioma cells through Src/epidermal growth factor receptor-mediated p38/Akt and phosphatidylinositol 3-kinase/Akt signaling pathways. Cancer Res. 66, 8511–8519.
[7] Wang, F., Liu, R., Lee, S.W., Sloss, C.M., Couget, J. and Cusack, J.C. (2007) Heparin-binding EGF-like growth factor is an early response gene to chemotherapy and contributes to chemotherapy resistance. Oncogene 26, 2006–2016.
[8] Winograd-Katz, S.E. and Levitzki, A. (2006) Cisplatin induces PKB/Akt activation and p38(MAPK) phosphorylation of the EGF receptor. Oncogene 25, 7381–7390.
[9] Benhar, M., Engelberg, D. and Levitzki, A. (2002) Cisplatin-induced activation of the EGF receptor. Oncogene 21, 8723–8731.
[10] Johnson, F.M., Saigal, B. and Donato, N.J. (2005) Induction of heparin-binding EGF-like growth factor and activation of EGF receptor in imatinib mesylate-treated squamous carcinoma cells. J. Cell. Physiol. 205, 218–227.
[11] Van Schaeybroeck, S., Kyula, J., Kelly, D.M., Karaiskou-McCaul, A., Stokesberry, S.A., Van Cutsem, E., Longley, D.B. and Johnston, P.G. (2006) Chemotherapy-induced epidermal growth factor receptor activation determines response to combined gefitinib/chemotherapy treatment in non-small cell lung cancer cells. Mol. Cancer Ther. 5, 1154–1165.
[12] Carpenter, G. (1987) Receptors for epidermal growth factor and other polypeptide mitogens. Annu. Rev. Biochem. 56, 881–914.
[13] Klapper, L.N., Kirschbaum, M.H., Sela, M. and Yarden, Y. (2000) Biochemical and clinical implications of the ErbB/HER signaling network of growth factor receptors. Adv. Cancer Res. 77, 25–79.
[14] Di Marco, E., Pierce, J.H., Fleming, T.P., Kraus, M.H., Molloy, C.J., Aaronson, S.A. and Di Fiore, P.P. (1989) Autocrine interaction between TGF alpha and the EGF-receptor: quantitative requirements for induction of the malignant phenotype. Oncogene 4, 831–838.
[15] Datta, S.R., Brunet, A. and Greenberg, M.E. (1999) Cellular survival: a play in three Akts. Genes Dev. 13, 2905–2927.
[16] Goswami, A., Ranganathan, P. and Rangnekar, V.M. (2006) The phosphoinositide 3-kinase/Akt1/Par-4 axis: a cancer-selective therapeutic target. Cancer Res. 66, 2889–2892.
[17] Katz, M., Amit, I. and Yarden, Y. (2007) Regulation of MAPKs by growth factors and receptor tyrosine kinases. Biochim. Biophys. Acta 1773, 1161–1176.
[18] Roberts, P.J. and Der, C.J. (2007) Targeting the Raf-MEK-ERK mitogen-activated protein kinase cascade for the treatment of cancer. Oncogene 26, 3291–3310.
[19] Yoshida, T., Okamoto, I., Okabe, T., Iwasa, T., Satoh, T., Nishio, K., Fukuoka, M. and Nakagawa, K. (2008) Matuzumab and cetuximab activate the epidermal growth factor receptor but fail to trigger downstream signaling by Akt or Erk. Int. J. Cancer 122, 1530–1538.

[20] Okabe, T., Okamoto, I., Tamura, K., Terashima, M., Yoshida, T., Satoh, T., Takada, M., Fukuoka, M. and Nakagawa, K. (2007) Differential constitutive activation of the epidermal growth factor receptor in non-small cell lung cancer cells bearing EGFR gene mutation and amplification. Cancer Res. 67, 2046–2053.
[21] Wu, L., Birle, D.C. and Tannock, I.F. (2005) Effects of the mammalian target of rapamycin inhibitor CCI-779 used alone or with chemotherapy on human prostate cancer cells and xenografts. Cancer Res. 65, 2825–2831.
[22] Akashi, Y., Okamoto, I., Iwasa, T., Yoshida, T., Suzuki, M., Hatashita, E., Yamada, Y., Satoh, T., Fukuoka, M., Ono, K. and Nakagawa, K. (2007) The novel microtubule-interfering agent TZT-1027 enhances the anticancer effect of radiation in vitro and in vivo. Br. J. Cancer 96, 1532–1539.
[23] Higashiyama, S. and Nanba, D. (2005) ADAM-mediated ectodomain shedding of HB-EGF in receptor cross-talk. Biochim. Biophys. Acta 1751, 110–117.
[24] Miyamoto, S., Yagi, H., Yotsumoto, F., Kawarabayashi, T. and Mekada, E. (2006) Heparin-binding epidermal growth factor-like growth factor as a novel targeting molecule for cancer therapy. Cancer Sci. 97, 341–347.
[25] Ono, M., Raab, G., Lau, K., Abraham, J.A. and Klagsbrun, M. (1994) Purification and characterization of transmembrane forms of heparin-binding EGF-like growth factor. J. Biol. Chem. 269, 31315–31321.
[26] Mitamura, T., Higashiyama, S., Taniguchi, N., Klagsbrun, M. and Mekada, E. (1995) Diphtheria toxin binds to the epidermal growth factor (EGF)-like domain of human heparin-binding EGF-like growth factor/diphtheria toxin receptor and inhibits specifically its mitogenic activity. J. Biol. Chem. 270, 1015–1019.
[27] Suganuma, K., Kubota, T., Saikawa, Y., Abe, S., Otani, Y., Furukawa, T., Kumai, K., Hasegawa, H., Watanabe, M., Kitajima, M., Nakayama, H. and Okabe, H. (2003) Possible chemoresistance-related genes for gastric cancer detected by cDNA microarray. Cancer Sci. 94, 355–359.
[28] Li, S., Schmitz, K.R., Jeffrey, P.D., Wiltzius, J.J., Kussie, P. and Ferguson, K.M. (2005) Structural basis for inhibition of the epidermal growth factor receptor by cetuximab. Cancer Cell 7, 301–311.
[29] Adams, G.P. and Weiner, L.M. (2005) Monoclonal antibody therapy of cancer. Nat. Biotechnol. 23, 1147–1157.
[30] Kleespies, A., Ischenko, I., Eichhorn, M.E., Seeliger, H., Amendt, C., Mantell, O., Jauch, K.W. and Bruns, C.J. (2008) Matuzumab short-term therapy in experimental pancreatic cancer: prolonged antitumor activity in combination with gemcitabine. Clin. Cancer Res. 14, 5426–5436.
[31] Graeven, U., Kremer, B., Sudhoff, T., Killing, B., Rojo, F., Weber, D., Tillner, J., Unal, C. and Schmiegel, W. (2006) Phase I study of the humanised anti-EGFR monoclonal antibody matuzumab (EMD 72000) combined with gemcitabine in advanced pancreatic cancer. Br. J. Cancer 94, 1293–1299.
[32] Rao, S., Starling, N., Cunningham, D., Benson, M., Wotherspoon, A., Lupfert, C., Kurek, R., Oates, J., Baselga, J. and Hill, A. (2008) Phase I study of epirubicin, cisplatin and capecitabine plus matuzumab in previously untreated patients with advanced oesophagogastric cancer. Br. J. Cancer 99, 868–874.
[33] Vanhoefer, U., Tewes, M., Rojo, F., Dirsch, O., Schleucher, N., Rosen, O., Tillner, J., Kovar, A., Braun, A.H., Trarbach, T., Seeber, S., Harstrick, A. and Baselga, J. (2004) Phase I study of the humanized antiepidermal growth factor receptor monoclonal antibody EMD72000 in patients with advanced solid tumors that express the epidermal growth factor receptor. J. Clin. Oncol. 22, 175–184.
[34] Salazar, R., Tabernero, J., Rojo, F., Jimenez, E., Montaner, I., Casado, E., Sala, G., Tillner, J., Malik, R. and Baselga, J. (2004) Dose-dependent inhibition of the EGFR and signalling pathways with the anti-EGFR monoclonal antibody (MAb) EMD 72000 administered every three weeks (q3w). A phase I pharmacokinetic/pharmacodynamic (PK/PD) study to define the optimal biological dose (OBD). J. Clin. Oncol. 22 (Suppl. 14), 127.
[35] Sirotnak, F.M., Zakowski, M.F., Miller, V.A., Scher, H.I. and Kris, M.G. (2000) Efficacy of cytotoxic agents against human tumor xenografts is markedly enhanced by coadministration of ZD1839 (Iressa), an inhibitor of EGFR tyrosine kinase. Clin. Cancer Res. 6, 4885–4892.

Int. J. Cancer: **124,** 1072–1080 (2009)

SRPX2 is overexpressed in gastric cancer and promotes cellular migration and adhesion

Kaoru Tanaka[1,2], Tokuzo Arao[1], Mari Maegawa[1], Kazuko Matsumoto[1], Hiroyasu Kaneda[1,2], Kanae Kudo[1], Yoshihiko Fujita[1], Hideyuki Yokote[1], Kazuyoshi Yanagihara[3], Yasuhide Yamada[4], Isamu Okamoto[2], Kazuhiko Nakagawa[2] and Kazuto Nishio[1]*

[1]*Department of Genome Biology, Kinki University School of Medicine, Osaka-Sayama, Osaka, Japan*
[2]*Department of Medical Oncology, Kinki University School of Medicine, Osaka-Sayama, Osaka, Japan*
[3]*Central Animal Lab, National Cancer Center Research Institute, Chuo-ku, Tokyo, Japan*
[4]*Department of Medical Oncology, National Cancer Center Hospital, Chuo-ku, Tokyo, Japan*

SRPX2 **(Sushi repeat containing protein, X-linked 2) was first identified as a downstream molecule of the *E2A-HLF* fusion gene in t(17;19)-positive leukemia cells and the biological function of this gene remains unknown. We found that *SRPX2* is overexpressed in gastric cancer and the expression and clinical features showed that high mRNA expression levels were observed in patients with unfavorable outcomes using real-time RT-PCR. The cellular distribution of SRPX2 protein showed the secretion of SRPX2 into extracellular regions and its localization in the cytoplasm. The introduction of the *SRPX2* gene into HEK293 cells did not modulate the cellular proliferative activity but did enhance the cellular migration activity, as shown using migration and scratch assays. The conditioned-medium obtained from SRPX2-overexpressing cells increased the cellular migration activity of a gastric cancer cell line, SNU-16. In addition, SRPX2 protein remarkably enhanced the cellular adhesion of SNU-16 and HSC-39 and increased the phosphorylation levels of focal adhesion kinase (FAK), as shown using western blotting, suggesting that SRPX2 enhances cellular migration and adhesion through FAK signaling. In conclusion, the overexpression of SRPX2 enhances cellular migration and adhesion in gastric cancer cells. Here, we report that the biological functions of SRPX2 include cellular migration and adhesion to cancer cells.**

Key words: SRPX2; gastric cancer; cellular adhesion; cellular migration

SRPX2 (Sushi repeat containing protein, X-linked 2) was first identified as *SRPUL* (Sushi repeat protein upregulated in leukemia) by Kurosawa *et al.*[1] The *E2A-HLF* fusion gene causes B-cell precursor acute lymphoblastic leukemia, which is characterized by an unusual paraneoplastic syndrome comprising intravascular coagulation and hypercalcemia; one of the target genes of *E2A-HLF* is *SRPX2*. Apart from the possible involvement of this gene in malignant diseases, a disease-causing mutation (p.N327S) in *SRPX2* resulting in a gain-of-glycosylation aberration in the secreted mutant protein, and the mutation actually leads to rolandic epilepsy with oral and speech dyspraxia and with mental retardation in the French family.[2] While a second mutation (p.Y72S) leads to rolandic epilepsy with bilateral perisylvian polymicrogyria in another family.[3] The involvement of *SRPX2* in these disorders suggests an important role for *SRPX2* in the perisylvian region, which is critical for language and cognitive development.

SRPX2 contains 3 sushi domains and 1 hyaline domain. A sushi domain, also known as a complement control protein module or a short complement-like repeat, contains ~60 amino acids and is found in functionally diverse proteins, such as regulators of the complement activation family, GABA receptor, thyroid peroxidase and selectin family.[4,5] Sushi domains are thought to mediate specific protein–protein or protein–carbohydrate binding and cellular adhesive functions.[4] A phylogenetic analysis revealed that *SRPX2* belongs to a family of 5 genes: *SRPX2*, *SRPX*, *SELP* (selectin P precursor), *SELE* (selectin E precursor) and *SVEP1* (selectin-like protein).[3] *SRPX/SRPX1/EXT1/DRS* has the highest degree of similarity and may be involved in X-linked retinitis pigmentosa.[6,7] The selectin family, which is well known for its biological roles in leukocyte migration, cellular attachment and rolling, also contains sushi domain repeats and are phylogenetic similar to *SRPX2*.[3]

SRPX2 also contains a hyaline (HYR) domain, and this domain probably corresponds to a new superfamily in the immunoglobulin fold. The HYR domains are often associated with sushi domains, and although the function of HYR domains is uncertain, it is thought to be involved in cellular adhesion.[8] Thus, accumulating data on the motifs found in *SRPX2* suggest that *SRPX2* may be involved in cellular adhesion.

We previously performed a microarray analysis of paired clinical samples of gastric cancer and noncancerous lesions obtained from gastric cancer patients[9] and found that *SRPX2* is overexpressed in gastric cancer tissue. The present study sought to clarify the biological function of *SRPX2* expression in gastric cancer.

Material and methods

Cell culture

HEK293 (human embryonic kidney cell line) was maintained in DMEM medium, and SNU-16, HSC-39, 44As3, HSC-43, HSC-44, MKN1 and MKN7 (human gastric cancer cell lines) were maintained in RPMI1640 medium (Sigma, St. Louis, MO) supplemented with 10% FBS (GIBCO BRL, Grand Island, NY). HUVEC (human umbilical vein endothelial cells) was maintained in Humedia-EG2 (KURABO, Tokyo, Japan) medium with 1% FBS under the addition of epidermal growth factor and fibroblast growth factor.

Expression vector construction and viral production

The full-length cDNA fragment encoding human *SRPX2* was obtained from 44As3 cells using RT-PCR and the following primers: SRPX2-F, CGG GAT CCT CAA GGA TGG CCA GTC AGC TAA CTC AAA GAG G; SRPX2-R, CCC AAG CTT GGG CTC GCA TAT GTC CCT TTG CTC CCG ACG CTG GG. The sequences of the PCR-amplified DNAs were confirmed by sequencing after cloning into a pCR-Blunt II-TOPO cloning vector (Invitrogen, Carlsbad, CA). *SRPX2* cDNA was fused to a GFP-containing pcDNA3.1 vector (Clontech, Palo Alt, CA). Empty, GFP and SRPX2-GFP vectors were then transfected into HEK293 cells using FuGENE6 transfection reagent (Roche Diagnostics, Basel, Switzerland). Hygromycin selection (100 μg/mL) was

Grant sponsors: Third-Term Comprehensive 10-Year Strategy for Cancer Control, The Program for the Promotion of Fundamental Studies in Health Sciences of the National Institute of Biomedical Innovation (NiBio), The Japan Health Sciences Foundation.

***Correspondence to:** Department of Genome Biology, Kinki University School of Medicine, 377-2 Ohno-higashi, Osaka-Sayama, Osaka 589-8511, Japan. Fax: +81-72-366-0206. E-mail: knishio@med.kindai.ac.jp

Received 18 June 2008; Accepted after revision 22 September 2008
DOI 10.1002/ijc.24065
Published online 22 October 2008 in Wiley InterScience (www.interscience.wiley.com).

performed on days 2–8 after transfection, and then the cells were cultured in normal medium for another 10 days. The vectors and stable transfectant HEK293 cells were designated as pcDNA-mock, pcDNA-GFP, pcDNA-SRPX2/GFP, HEK293-pcDNA-mock, HEK293-pcDNA-GFP and HEK293-pcDNA-SRPX2/GFP.

SRPX2 cDNA in pcDNA3.1 vector was cut out and transferred into a pQCLIN retroviral vector (BD Biosciences Clontech, San Diego, CA) together with enhanced green fluorescent protein (EGFP) following internal ribosome entry site sequence (IRES) to monitor the expression of the inserts indirectly. A pVSV-G vector (Clontech, Palo Alt, CA) for the constitution of the viral envelope and the pQCXIX constructs were cotransfected into the GP2-293 cells using FuGENE6 transfection reagent. Briefly, 80% confluent cells cultured on a 10-cm dish were transfected with 2 μg pVSV-G plus 6 μg pQCXIX vectors. After 48 hr of transfection, the culture medium was collected and the viral particles were concentrated by centrifugation at 15,000*g* for 3 hr at 4°C. The viral pellet was then resuspended in fresh RPMI1640 medium. The titer of the viral vector was calculated by counting the EGFP-positive cells that were infected by serial dilutions of virus-containing media, and the multiplicity of infection (MOI) was then determined. The viral vector and stable viral transfectant cells in each cell line were designated as pQCLIN-EGFP, pQCLIN-SRPX2, HEK293-pQCLIN-EGFP, HEK293-pQCLIN-SRPX2, MKN1-pQCLIN-EGFP and MKN1-pQCLIN-SRPX2.

Patients and samples

An analysis of *SRPX2* expression levels and clinical features was performed using data from patients aged 20 to 75 years and with histologically confirmed, Stage IV gastric cancer. Additional inclusion criteria included an Eastern Cooperative Oncology Group performance status of 0–2. The exclusion criteria included prior chemotherapy or major surgery. Fifty-seven gastric cancer samples were evaluated in this study. All the patients received chemotherapy after registration and endoscopical biopsy. Gastric cancer and noncancerous gastric mucosa samples were evaluated for *SRPX2* expression in the first consecutive 24 patients. This study was approved by the institutional review board of the National Cancer Center Hospital, and written informed consent was obtained from all the patients. Endoscopic biopsy samples were immediately placed in an RNA stabilization solution (Isogen; Nippongene, Tokyo, Japan) and stored at −80°C. Other biopsy samples obtained from the same location were reviewed by a pathologist to confirm the presence of tumor cells. The RNA extraction method and the quality check protocol have been previously described.[10]

Real-time reverse-transcription PCR

One microgram of total RNA from normal tissue purchased from Clontech and from a cultured cell line was converted to cDNA using a GeneAmp® RNA-PCR kit (Applied Biosystems, CA). Real-time PCR was carried out using the Applied Biosystems 7900HT Fast Real-time PCR System (Applied Biosystems) under the following conditions: 95°C for 6 min, 40 cycles of 95°C for 15 sec and 60°C for 1 min. Glyceraldehyde 3 phosphate dehydrogenase (*GAPD*, NM_002046) was used to normalize the expression levels in the subsequent quantitative analyses. To amplify the target genes, the following primers were purchased from TaKaRa (Yotsukaichi, Japan): SRPX2-FW, ACT GGA TTT GCG GCA TGT GA; SRPX2-RW, CCA TGT TGA AGT AGG AGC GAG TGA; GAPD-FW, GCA CCG TCA AGG CTG AGA AC; GAPD-RW, ATG GTG GTG AAG ACG CCA GT.

Anti-SRPX2 polyclonal antibody

Rabbit antibodies specific for SRPX2 were obtained by immunizing rabbits with SRPX2 peptide (FIDDYLLSNQELTQ) according to a previously described method,[2] and IgG was purified from serum using standard protocols.

SRPX2-conditioned medium

The media in which subconfluent HEK293-pQCLIN-EGFP, HEK293-pQCLIN-SRPX2, MKN1-pQCLIN-EGFP and MKN1-pQCLIN-SRPX2 cells were being cultured was replaced with a serum-reduced medium (OPTI-MEM; GIBCO), the cells were cultured for an additional 24 hr and the conditioned-media were collected. The media were filtered using Millex-GS (Millipore, Bedford, MA) and concentrated using the Amicon Ultra (Millipore) and stored at −80°C. The concentration of the conditioned-medium was measured using a BCA protein assay (Pierce Biotechnology, Rockford, IL) and equalized.

Western blot analysis

The antibodies used in this study were anti-GFP (Invitrogen, Carlsbad, CA), anti-focal adhesion kinase (anti-FAK), anti-p-FAK (pY397) (BD Biosciences), anti-β-actin (Santa Cruz Biotechnology, Santa Cruz, CA) and anti-p-FAK (pY576/577) (Cell Signaling, Beverly, MA).

A Western blot analysis was performed as described previously (Ref. 10). In brief, subconfluent cells were washed with cold phosphate-buffered saline (PBS) and harvested with Lysis A buffer containing 1%Triton X-100, 20 mM Tris-HCl (pH 7.0), 5 mM EDTA, 50 mM sodium chloride, 10 mM sodium pyrophosphate, 50 mM sodium fluoride, 1 mM sodium orthovanadate and a protease inhibitor mix, complete™ (Roche Diagnostics). Whole-cell lysates and culture medium were separated using a 2–15% gradient SDS-PAGE and blotted onto a polyvinylidene fluoride membrane. After blocking with 3% bovine serum albumin in a TBS buffer (pH 8.0) with 0.1% Tween-20, the membrane was probed with primary antibody. After rinsing twice with TBS buffer, the membrane was incubated with horseradish peroxidase-conjugated secondary antibody (Cell Signaling) and washed followed by visualization using an ECL detection system (Amersham) and LAS-3000 (Fujifilm, Tokyo, Japan). The data were quantified by automated densitometry using Multigauge Ver 3.0 (Fujifilm).The experiment was performed in triplicate.

Cellular growth assay

HEK293 transfectant cells were incubated on 96-well plates at a density of 2000/well with 180 μL of culture medium at 37°C in 5% CO_2. After 24, 48 or 72 hr of incubation, 20 μL of MTT [3-(4,5-dimethyl-thiazoyl-2-yl)2,5-diphenyltetrazolium bromide] solution (SIGMA) was added and the cultures were incubated for 4 hr at 37°C. After centrifugation, the culture medium was discarded and the wells were filled with DMSO. The absorbance of the cultures at 562 nm was measured using VERSAmax (Japan Molecular Devices, Tokyo, Japan). The experiment was performed in triplicate.

Cellular adhesion assay

EGFP-conditioned or SRPX2-conditioned media obtained from HEK293-pQCLIN-EGFP, HEK293-pQCLIN-SRPX2, MKN1-pQCLIN-EGFP or MKN1-pQCLIN-SRPX2 cells were adjusted to a concentration of 1 mg/mL and 50 μL were incubated at 4°C overnight on 96-well plates. The conditioned media were aspirated, and the wells were washed twice with PBS. The plates were then used in an adhesion assay as conditioned medium-coated 96-well plates. The cells to be analyzed were added to the wells of conditioned medium-coated plates (2×10^4 cells /well) and incubated at 37°C for 1 hr. When treated with FAK inhibitors (PP2 and Herbimycin A; Calbiochem, San Diego, CA), the cells to be analyzed were incubated for 4 hr. The wells were then washed twice with PBS to remove nonadherent cells. Adherent cells were evaluated using the MTT assay as described above. The average O.D. values of 3 wells were used for a single experiment, and the experiment was performed in triplicate.

Migration assay and chemotaxis assay

Migration assays were performed using the Boyden-chamber methods and polycarbonate membranes with an 8-μm pore size

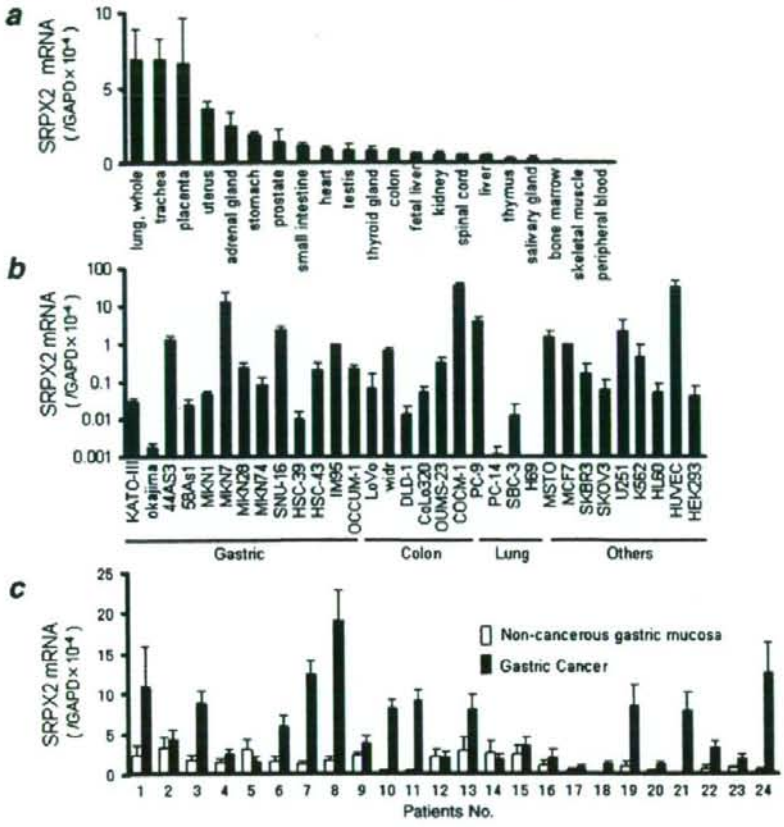

FIGURE 1 – Tissue distribution of *SRPX2* mRNA expression. The mRNA expression levels of *SRPX2* were determined using a real-time RT-PCR analysis in (*a*) human normal tissue; (*b*) 30 human cancer cell lines, HEK293 and HUVEC cell lines and (*c*) paired clinical samples that were endoscopically obtained from gastric cancer and the noncancerous gastric mucosa of the same patients. *GAPD* was used to normalize the expression levels in the subsequent quantitative analyses. The mRNA expression levels of *SRPX2* were significantly higher in the gastric cancer lesions ($p = 0.0004$). Error bars represent the SDs of 3 independent experiments. [Color figure can be viewed in the online issue, which is available at www.interscience.wiley.com.]

(chemotaxicell; KURABO). The membranes were coated with fibronectin on the outer side and dried for 2 hr at room temperature. The cells to be analyzed (2×10^4/well) were then seeded onto the upper chambers with 200 μL of migrating medium (DMEM containing 0.5% FBS), and the upper chambers were placed into the lower chambers of 24-well culture dishes containing 600 μL of DMEM containing 10% FBS. After incubation for 8 hr at 37°C, the media in the upper chambers were aspirated and the nonmigrated cells on the inner sides of the membranes were removed using a cotton swab. The cells that had migrated to the outer side of the membranes were fixed with 4% paraformaldehyde for 10 min and stained with 0.1% crystal violet for 15 min, then counted using a light microscope. The experiment was performed in triplicate.

The chemotaxis assays were performed using SNU-16 cells. A total of 1×10^5 cells were seeded onto the upper chambers with 200 μL of RPMI containing 0.5% FBS. The final concentration at 100 μg/mL of EGFP-conditioned or SRPX2-conditioned medium was added to the 600 μL volume of RPMI1640 containing 0.5% FBS medium in the lower chamber of the 24-well culture dishes. The cells were then incubated for 24 hr at 37°C with 5% CO_2. The number of migrated cells was evaluated as described earlier. The experiment was performed in triplicate.

Wound healing assay

HEK293-pQCLIN-EGFP and HEK293-pQCLIN-SRPX2 cells were plated onto 3.5-cm dishes and incubated in DMEM containing 10% FBS until they reached confluence. Wounds were introduced to the confluent cell monolayer using a plastic pipette tip. The cells were then cultured with DMEM containing 10% FBS at 37°C. After 4, 8 and 12 hr later, the wound area was photographed using a light microscope and measured. The experiment was performed in triplicate.

Fluorescent microscopy

HEK293-pcDNA-GFP and HEK293-pcDNA-SRPX2/GFP cells were treated with DAPI (6-diamidino-2-phenylindole) to stain the nucleus and photographed using fluorescent microscopy, IX71 (Olympus, Tokyo, Japan).

Statistics

The *t* test was used for comparison between 2 groups and paired *t* test was used for paired-samples in Figure 1*c*. The statistical analysis was performed using Excel software (Microsoft, Redmond, WA). A p value < 0.05 was considered significant.

Results

Tissue distribution of SRPX2 mRNA in normal tissues and cell lines

To examine the tissue distribution of *SRPX2* mRNA, we performed real-time RT-PCR for 24 normal human tissues. High expression levels of *SRPX2* mRNA were detected in the placenta, lung, trachea, uterus and adrenal gland, whereas the levels in the peripheral blood, brain and bone marrow were relatively low (Fig. 1*a*). Combined with data from previous reports,[1,2] *SRPX2* mRNA